Modeling epidemics:
from Bernoulli-d'Alembert model to modern approaches

Example of the Covid-19 outbreak modelling

J. Demongeot
UGA & IUF

Daniel Bernoulli’s life

February 9th 1700 (Groningen, NL) – March 17th 1782 (Basel, Switzerland)

- Learning differential calculus of Leibnitz, with his father Jean and uncle Jacques (student of Leibnitz)
- Receiving a M.D. degree (1721), after studying philosophy, logic, and medicine at universities of Heidelberg, Strasbourg, and Basel
- Lecturing in St Petersburg until 1732, in medicine, mechanics, and physics
- Returning to University of Basel, and accepting a post in anatomy and botany.

Bernoulli D (1760). Essai d'une nouvelle analyse de la mortalité causée par la petite vérole, et des avantages de l'inoculation pour la prévenir. Paris: Acad. Roy. Sci.

States variables

Population divided into: **susceptible *U***, *not yet been infected,* **infected λ** *and* **immune *W***, *immunized for the rest of their life after one infection.*

- ***u(a):*** *probability for a newborn individual to be susceptible (and alive) at age a.*

$$S(a) = U(a) + \lambda(a) + W(a)$$

- ***w(a):*** *probability to be immune (and alive) at age a.*

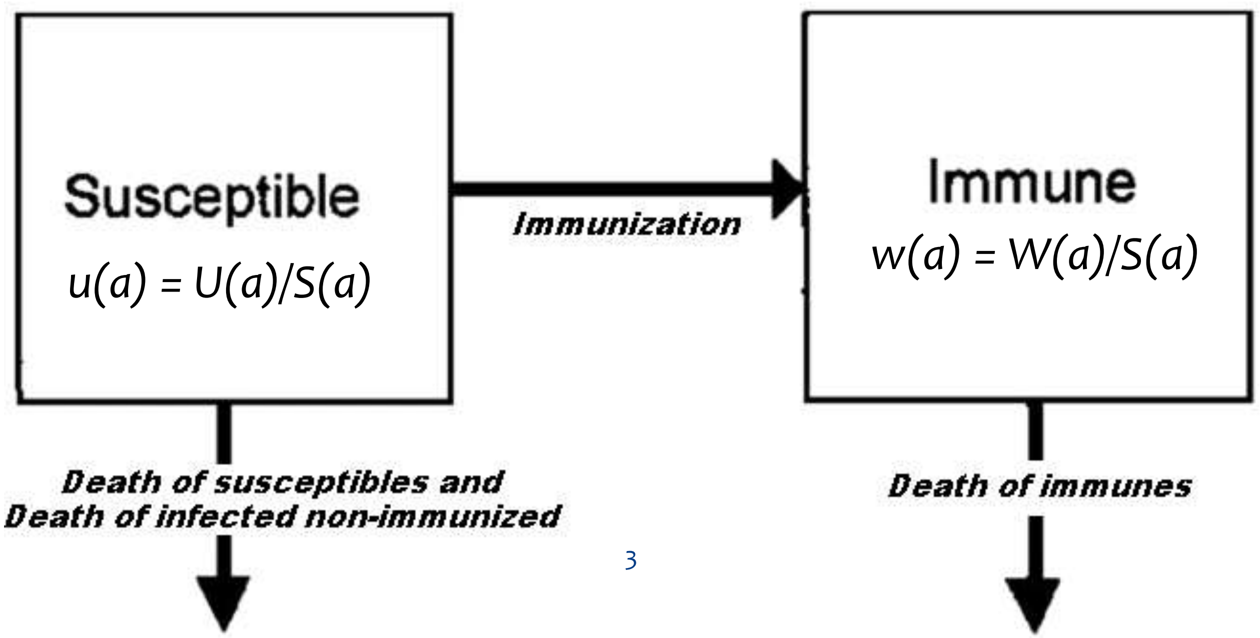

Differential equations

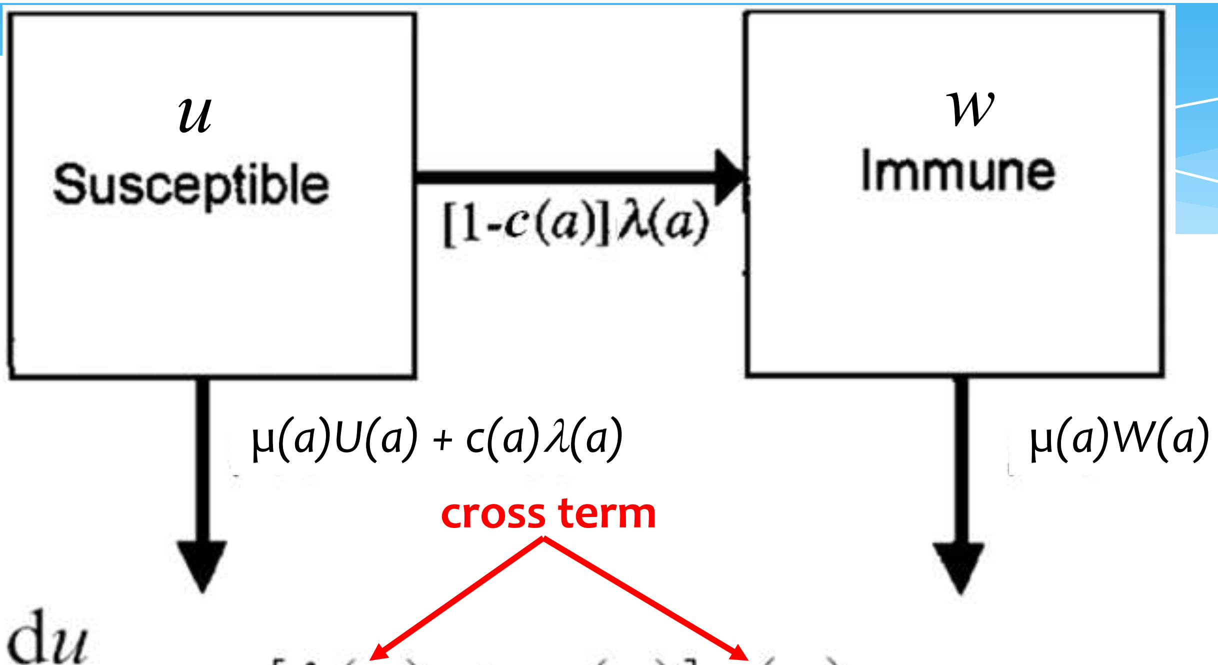

$$\frac{du}{da} = -[\lambda(a) + \mu(a)]u(a)$$

$$\frac{dw}{da} = [1 - c(a)]\lambda(a)u(a) - \mu(a)w(a)$$

SIRS model
Ross (1916) & McKendrick (1925)

Ronald Ross

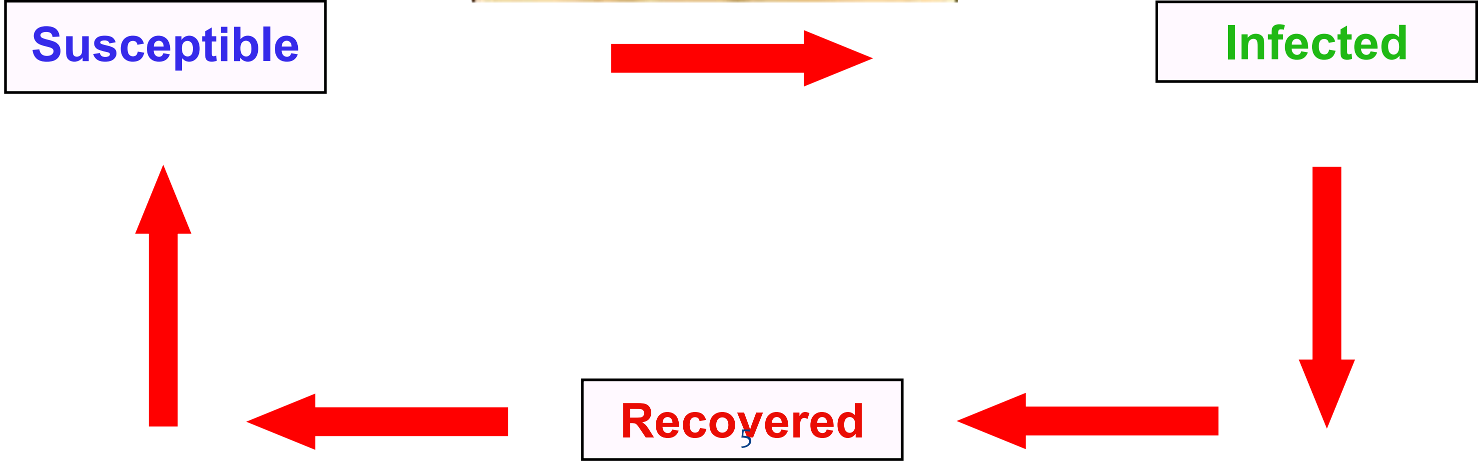

Susceptible

Infected

Recovered

The SIRS model

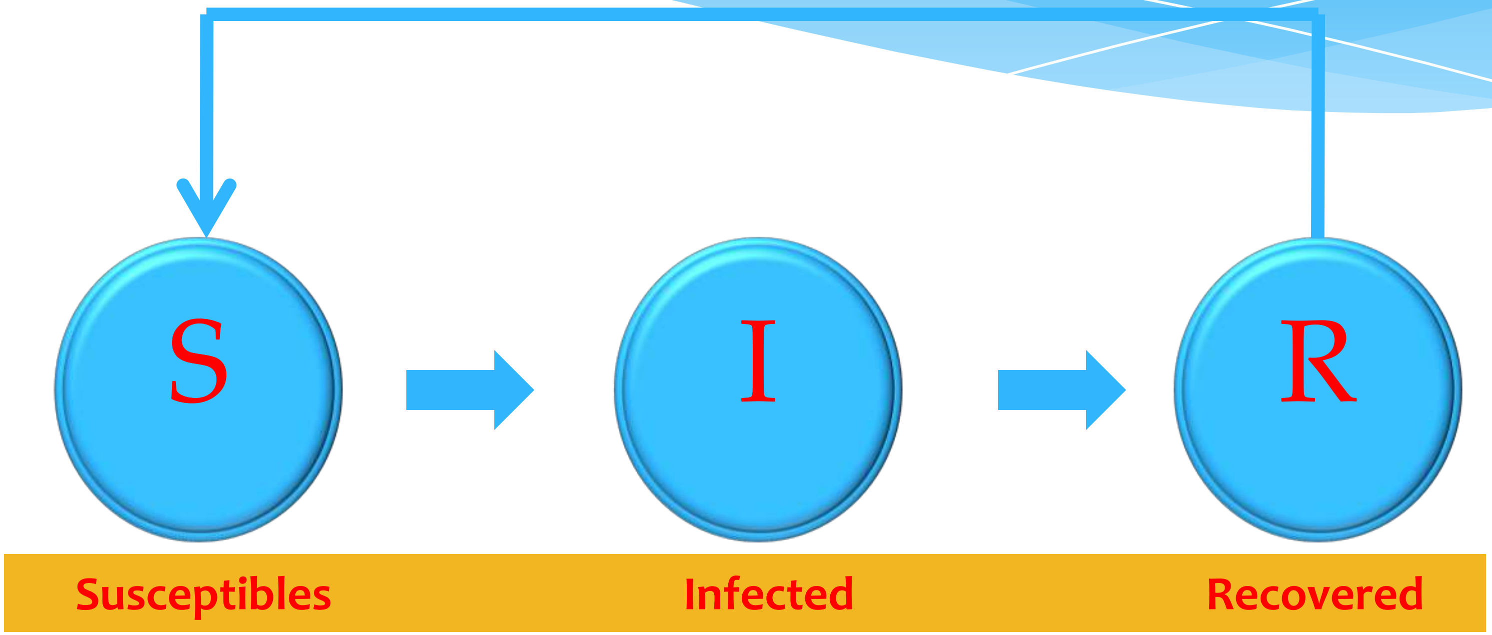

The SIRS model allows for a loss of immunity causing recovered individuals to become susceptible again.

Probabilistic approach

At least one event (contact ν, birth f, death μ) in (t, t+dt), and, if $I=N-S$:

$$P(S(t+dt)=k) = (1-\nu k(N-k)dt)\, P(S(t)=k) + f dt\, P(S(t)=k-1) - \mu dt\, P(S(t)=k+1)$$

By multipyling by s^k and summing over k, we prove, **if S and I are independent**, that they are Poisson, whose expectation E(S) verifies (by multiplying by k and summing over k):

$$dE(S)/dt \approx f\,E(S) - \nu\,E(SI) - \mu E(S)$$
$$\approx -\nu\,E(S)\,E(I), \text{ if } f = \mu$$

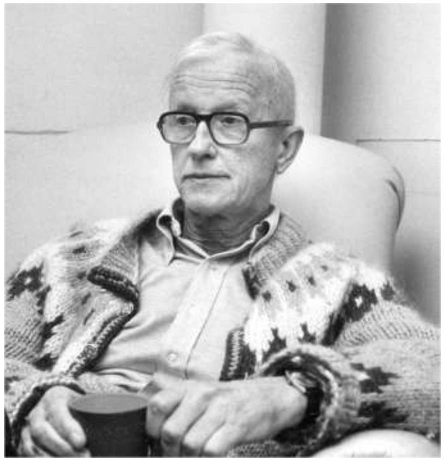

M. Delbrück 1940

Stability parameters =

1) Dominant eigenvalue of ODE's Jacobian matrix (Malthus)

3) KS evolutionary entropy of the Markov process (Demetrius)

M. Delbrück. Statistical fluctuations in autocatalytic reactions. *Journal of Chemical Physics* **8,** 120–124 (1940)

C.J. Rhodes & L. Demetrius. Evolutionary entropy determines invasion success in emergent epidemics. *PloS ONE*, **5,** e12951 (2010).

J. Demongeot & L. Demetrius. Complexity and Stability in Biological Systems. *Int. J. Bifurcation & Chaos*, **25,** 40013 (2015).

If at least one event (contact ν, birth f, death μ or recovering ρ) occurs in $(t, t+\mathrm{d}t)$, we have if births compensate deaths, leaving constant the total size N of the population:

$$\begin{aligned}P(S(t+\mathrm{d}t)=k, I(t+\mathrm{d}t)=N-k) = {} & (1 - [\mu k + \nu k(N-k) - fk - \rho(N-k)]\mathrm{d}t)\, P(S(t)=k, I(t)=N-k) \\ & + [f(k-1)+\rho(N-k+1)]\mathrm{d}t\, P(S(t)=k-1, I(t)=N-k+1) \\ & - [\mu(k+1) + \nu(k+1)(N-k-1)]\mathrm{d}t\, P(S(t)=k+1, I(t)=N-k-1)\end{aligned}$$

Hence, we have:

$$\begin{aligned}\mathrm{d}P(S(t)=k, I(t)=N-k)/\mathrm{d}t = {} & [P(S(t+\mathrm{d}t)=k, I(t+\mathrm{d}t)=N-k) - P(S(t)=k, I(t)=N-k)]/\mathrm{d}t = \\ & - [\mu k + \nu k(N-k) - fk - \rho(N-k)]\, P(S(t)=k, I(t)=N-k) \\ & + [f(k-1)+\rho(N-k+1)]\, P(S(t)=k-1, I(t)=N-k+1) \\ & - [\mu(k+1)+ \nu(k+1)(N-k-1)]\, P(S(t)=k+1, I(t)=N-k-1),\end{aligned}$$

and, if $P_k(t)$ denotes $P(S(t)=k, I(t)=N-k)$:

$$\begin{aligned}\mathrm{d}P_k(t)/\mathrm{d}t = {} & -[\mu k + \nu k(N-k) - fk - \rho(N-k)]\, P_k(t) + [f(k-1) + \rho(N-k+1)]\, P_{k-1}(t) \\ & - [\mu(k+1)+ \nu(k+1)(N-k-1)]\ \ P_{k+1}(t)\end{aligned}$$

Then, by multipyling by s^k and summing over k, we obtain the characteristic function of the random variable S, which is proven to be a Poisson random variable if the parameters ν, f, μ and ρ are sufficiently small. If births do not compensate deaths, we have:

$$\begin{aligned}P(S(t+\mathrm{d}t)=k, I(t+\mathrm{d}t)=j) = {} & (1 - [\mu k + \nu kj - fk - \rho j]\mathrm{d}t)\, P(S(t)=k, I(t)=j) \\ & + [f(k-1)+\rho(j+1)]\mathrm{d}t\, P(S(t)=k-1, I(t)=j+1) \\ & - [\mu(k+1) + \nu(k+1)(j-1)]\mathrm{d}t\, P(S(t)=k+1, I(t)=j-1)\end{aligned}$$

The SIRS Model Equations

$$dS/dt = fS - \nu SI - \mu S + \gamma R$$

$$dI/dt = \nu SI - cI - (1-c)I$$

$$dR/dt = (1-c)I - \gamma R$$

Bernoulli, 1760
d’Alembert, 1761
Lambert, 1772

Delbrück, 1940

Bartholomay, 1958

McQuarrie, 1967

Gillespie, 1970

Multi-agent or IBM discrete stochastic models

Verhulst, 1838

Ronald Ross, 1916

McKendrick, 1925
Dr Pasteur Institute Kausali

Ronald Fisher & KPP, 1937

ODE or PDE continuous deterministic models

Ro

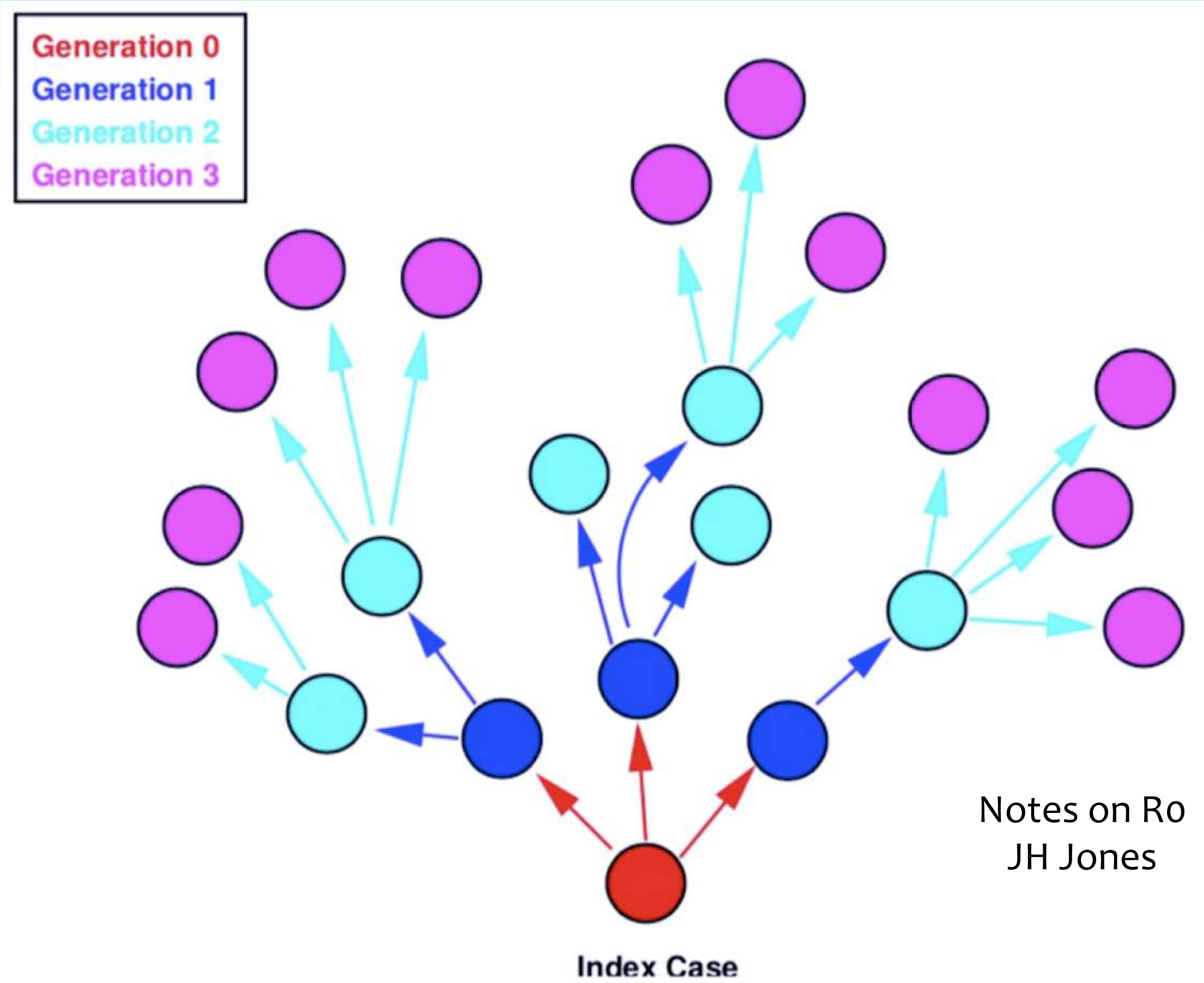

Notes on Ro
JH Jones

R_0

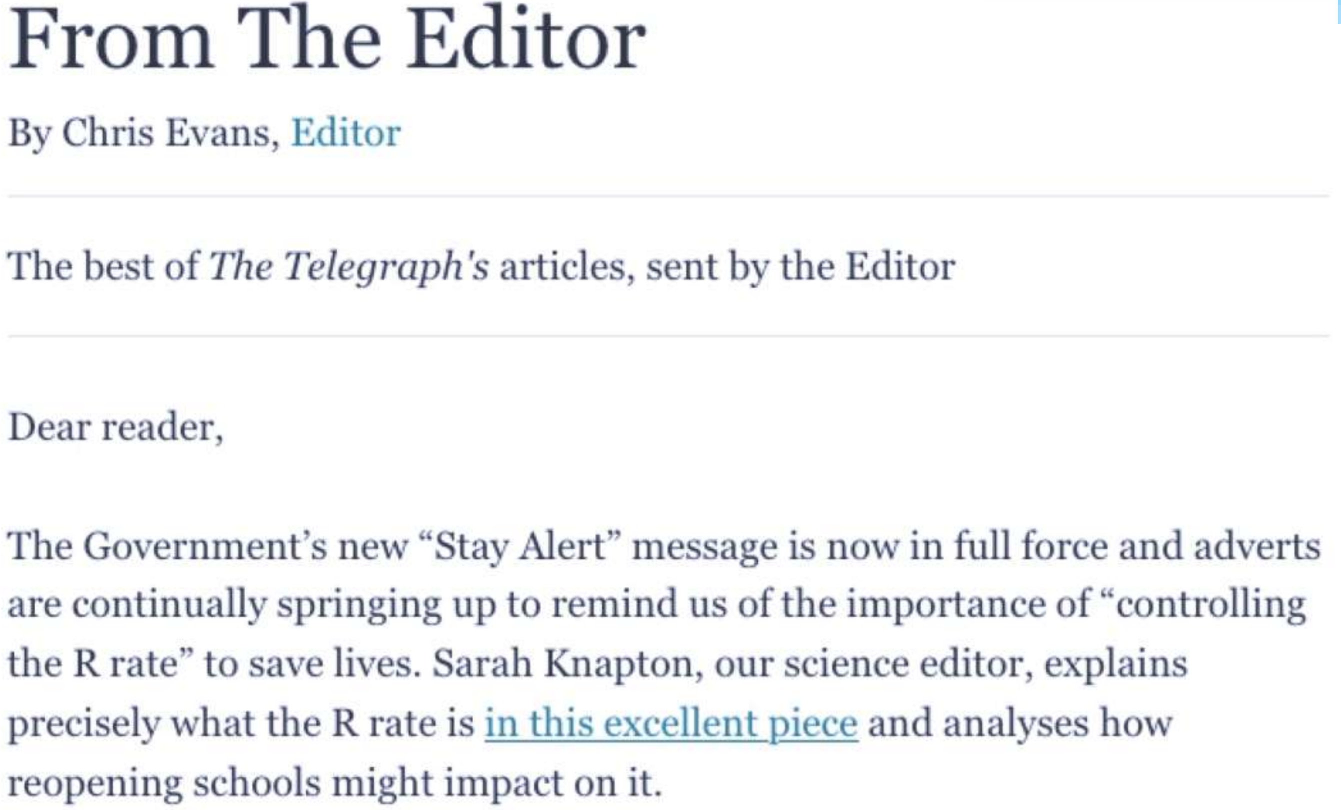

From The Editor

By Chris Evans, Editor

The best of *The Telegraph's* articles, sent by the Editor

Dear reader,

The Government's new "Stay Alert" message is now in full force and adverts are continually springing up to remind us of the importance of "controlling the R rate" to save lives. Sarah Knapton, our science editor, explains precisely what the R rate is [in this excellent piece]() and analyses how reopening schools might impact on it.

R_0

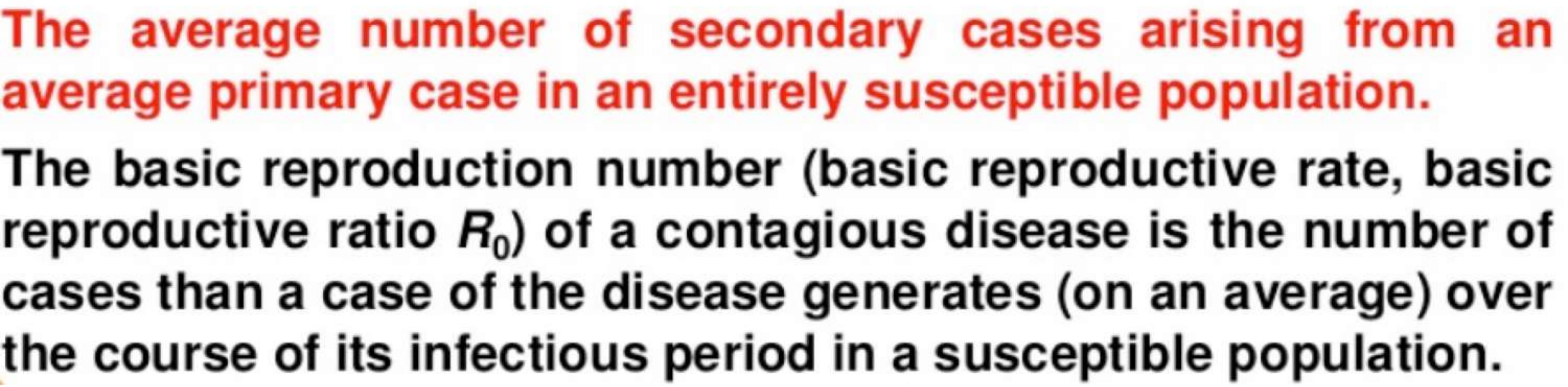

The average number of secondary cases arising from an average primary case in an entirely susceptible population.

The basic reproduction number (basic reproductive rate, basic reproductive ratio *R_0*) of a contagious disease is the number of cases than a case of the disease generates (on an average) over the course of its infectious period in a susceptible population.

- If $a \ll 1$, then $dI/dt = \nu SI$, $d\mathrm{Log}I/dt = \nu S$, and if $I(0) = 1$ and S is quasi-constant (equal to $\underline{S}$) at start of the epidemics:

$$\mathrm{Log}(I(t)) = \nu \int_{[0,\tau]} S(\tau)d\tau \approx \nu \underline{S} t \,,$$

$$\text{if } \mathrm{Log}(I(t)) \approx \mathrm{Log}(R_0)t, \text{ then}$$

$$R_0 \approx e^{\nu \underline{S}} \approx 1+\nu \underline{S}, \text{ if } \nu \underline{S} \ll 1$$

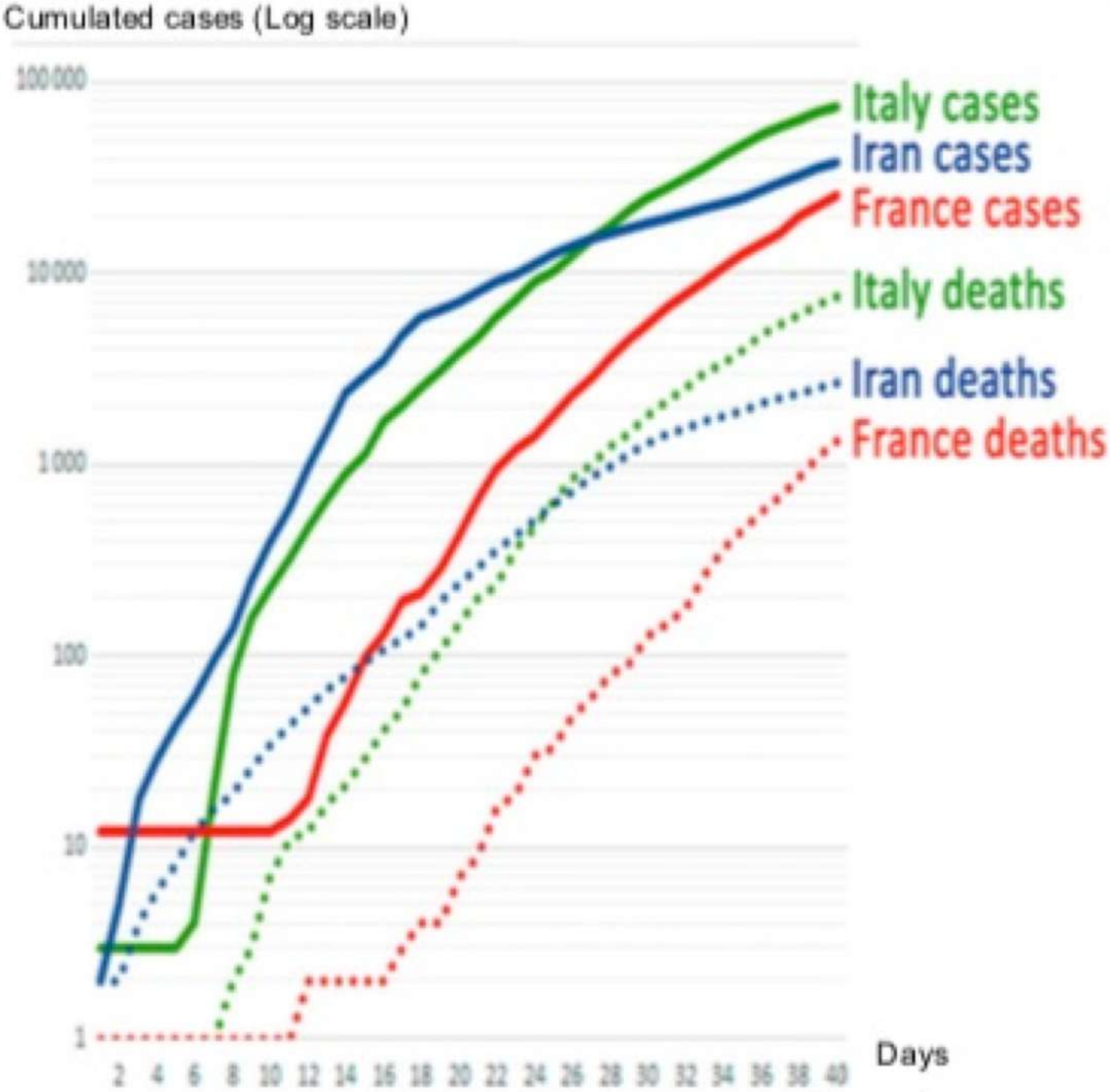
Cumulated cases (Log scale)
100 000
10 000
1 000
100
10
1
2
4
6
8
10
12
14
16
18
20
22
24
26
28
30
32
34
36
38
40
Days
Italy cases
Iran cases
France cases
Italy deaths
Iran deaths
France deaths

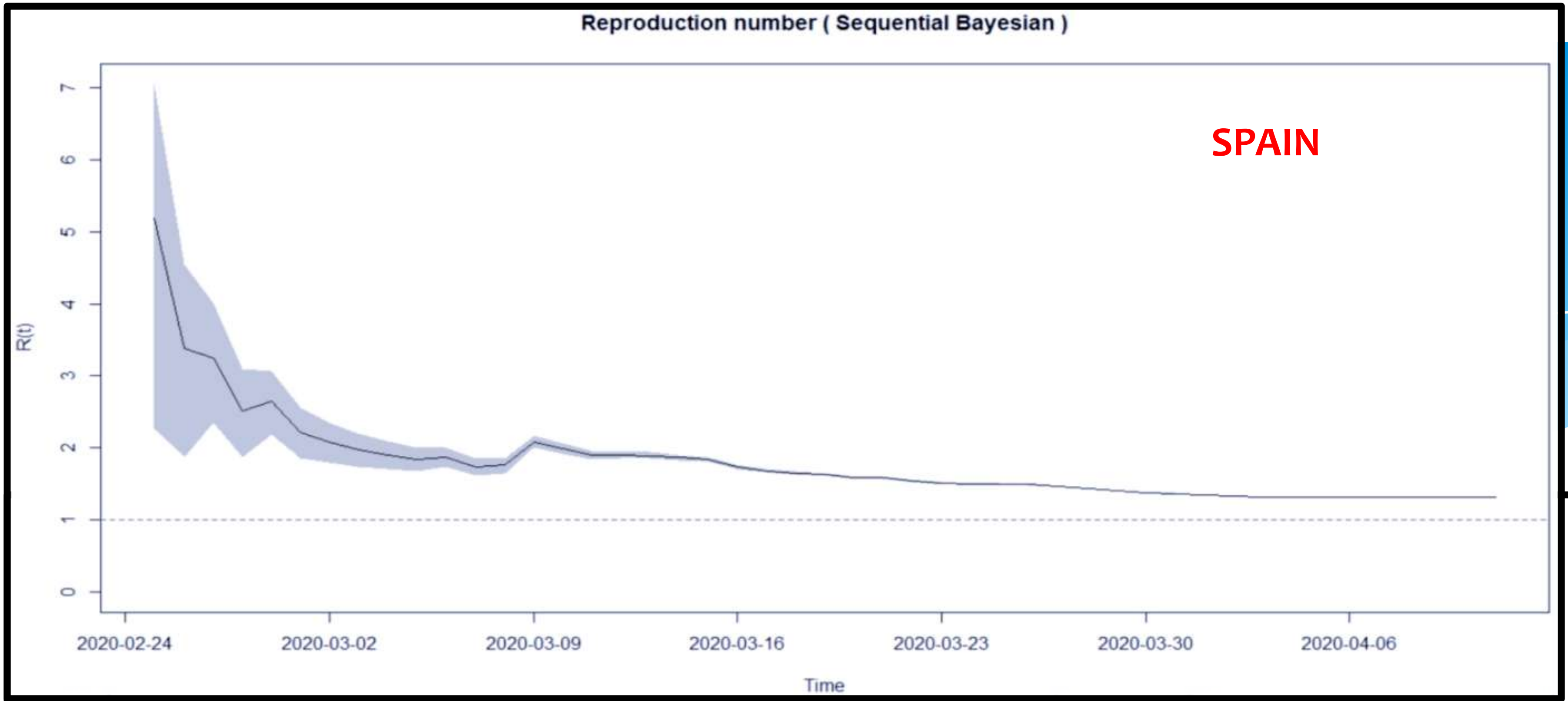
Reproduction number (Sequential Bayesian)
R(t)
0
1
2
3
4
5
6
7
2020-02-24
2020-03-02
2020-03-09
2020-03-16
2020-03-23
2020-03-30
2020-04-06
Time

SPAIN

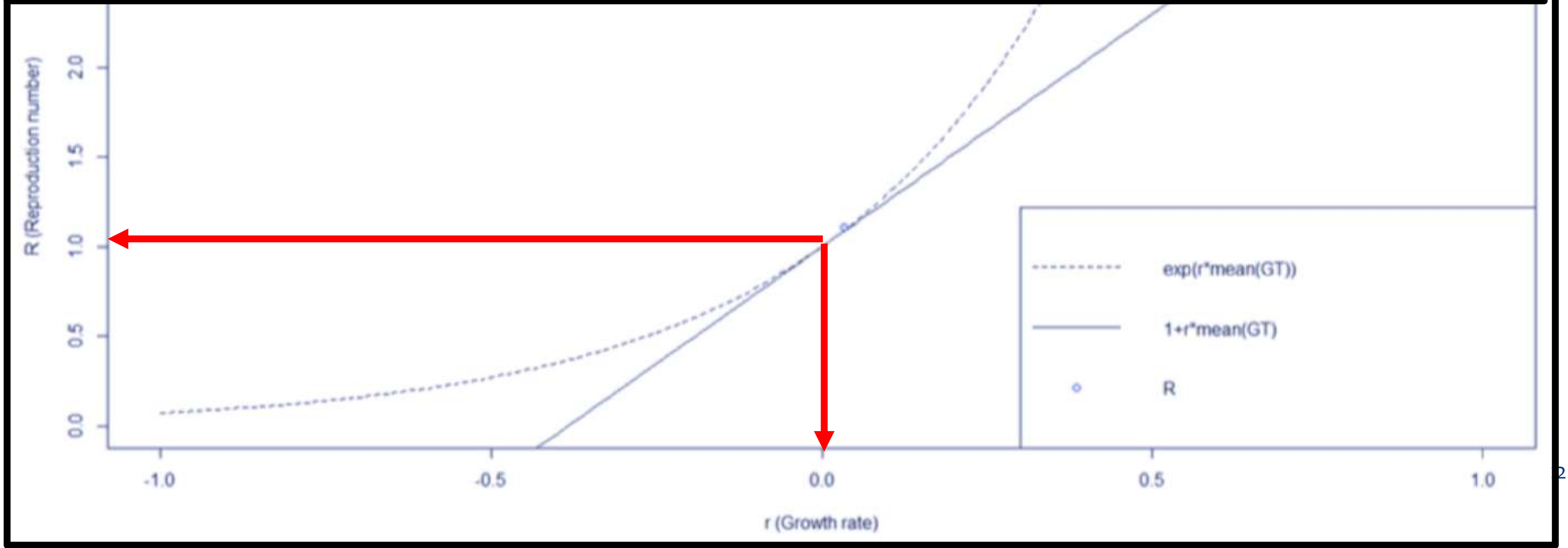
R (Reproduction number)
0.0
0.5
1.0
1.5
2.0
-1.0
-0.5
0.0
0.5
1.0
r (Growth rate)
exp(r*mean(GT))
1+r*mean(GT)
R

Restrictions :

- If S(0) is very large and I(0) small, then let use a saturation term rSI/(1+S)
- If the total population remains stable (f=μ), then S+I=N and S and I are not independent
- If the population is heterogeneous (e.g., if infectivity and susceptibility depends on age), then R_0 does not represent the initial exponential growth rate of infected

R_0 depends on the day of the contagion period

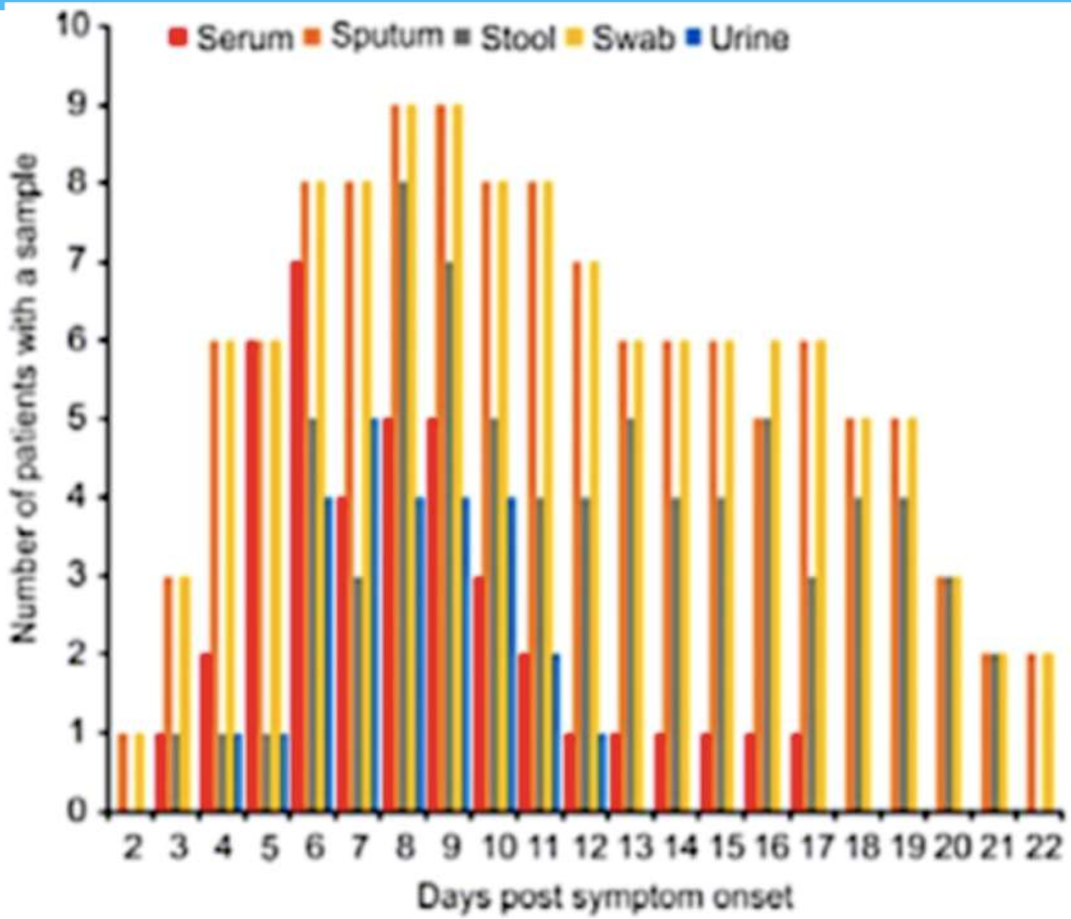

J. Demongeot, Y. Flet-Berliac & H. Seligmann Temperature decreases spread parameters of the new covid-19 cases dynamics. *Biology (Basel)*, **9,** 94 (2020).

Modèle auto-régressif ARp

On dit que (X_t) est un processus **auto-régressif d'ordre** p (centré) s'il s'écrit

$$X_t = \epsilon_t + \sum_{j=1}^{p} a_j X_{t-j}, \tag{1}$$

où ϵ_t est un bruit blanc centré de variance σ^2.

X_t est alors :

- la somme d'un choc aléatoire à l'instant t, ϵ_t, indépendant de l'historique
- d'une fonction linéaire de son passé $\sum_{j=1}^{p} a_j X_{t-j}$

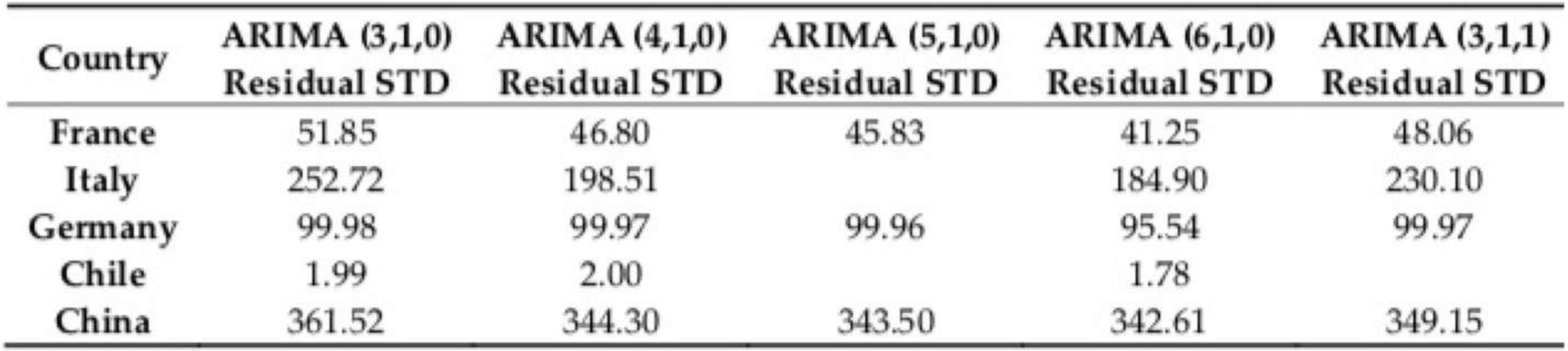

Country	ARIMA (3,1,0) Residual STD	ARIMA (4,1,0) Residual STD	ARIMA (5,1,0) Residual STD	ARIMA (6,1,0) Residual STD	ARIMA (3,1,1) Residual STD
France	51.85	46.80	45.83	41.25	48.06
Italy	252.72	198.51		184.90	230.10
Germany	99.98	99.97	99.96	95.54	99.97
Chile	1.99	2.00		1.78	
China	361.52	344.30	343.50	342.61	349.15

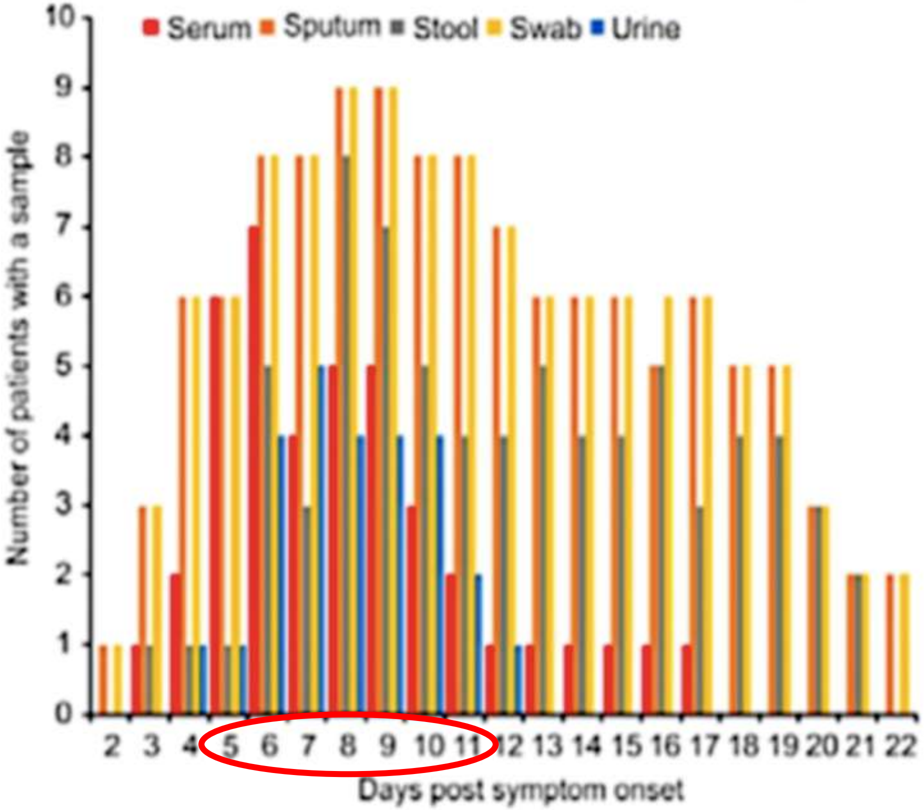

J. Demongeot, Y. Flet-Berliac & H. Seligmann Temperature decreases spread parameters of the new covid-19 cases dynamics. *Biology (Basel)*, **9,** 94 (2020).

If the model is deterministic, if X_j denotes the number of new cases at day j, and if the contagious period is made of r consecutive days, with R_k the marginal reproduction rate at day k of the contagious period, we have:

$$X_j = S_{k=1,r} R_k X_{j-k}$$

It is easy to show that, if $X_0 = 1$ and r=5:

$$X_5 = R_1^5 + 4R_1^3R_2 + 3R_1^2R_3 + 3R_1R_2^2 + 2R_2R_3 + 2R_1R_4 + R_5$$

If R_2 et R_3 are dominant and equal to R/2, then X_5 behaves as $2R_2R_3 = R^2/2$; More generally, If R1 = a, R_2 = b and R_3 = c, we get:

$$X_7 = a^7 + 6a^5b + 5a^4c + 10a^3b^2 + 12\,a^2bc + 4ab^3 + 3b^2c + 3ac^2, \text{etc.}$$

If R_2 and R_3 equal respectively a and b, and if a=b=R/2, c=0, then X_5 behaves like:

$$X_5 = R^5/32 + R^4/4 + 3R^3/8$$

If R = 1, $\{X_j\}_{i=1,\infty}$ is the Fibonacci sequence, and more generally, the generalized Fibonacci one.

Suppose that b = 0 and a depends on the day j: $a_j = aC(j)$, where C(j) represents the number of possible susceptibles recruitable by infectious at day j. If cumulated infected individuals (supposed to be all infectious) at day j are denoted by I_j, we have:

$$X_j = \Delta I_j/\Delta i = I_j - I_{j-1} = aC(j)I_{j-1}$$

Suppose that the first infected are recruited at the center of its sphere of influence and that the secondary infected individuals remain in this sphere, by widening the radius on day j, therefore the susceptibles C (j), where each infected on day j- 1 recruits a decreasing part of the sphere of influence:

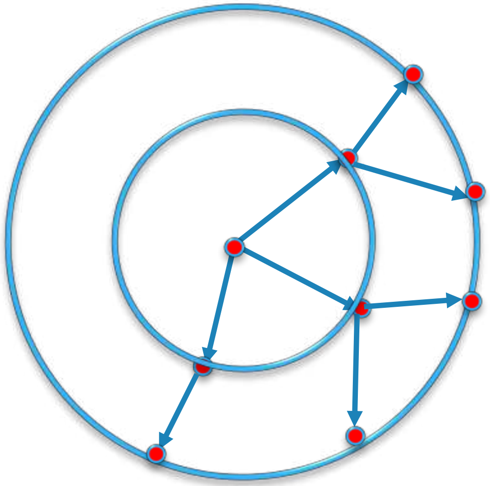

The function C(j) decreases due to the bulk on the successive spheres and we can consider the following functional form C(j)= S(j)/(c+S(j)), where S(j) is the number of susceptibles at day j.

Then, we can write the following equation taking into account the mortality:

$$X_j = \Delta I_j/\Delta i = aC(j)I_{j-1} = a\, I_{j-1}\, S(j)/(c+S(j)) - \mu I_{j-m},$$

The corresponding continuous equation is close to the SIR equation, if c is great before *S*:

$$dI/dt = aIS/(c+S) - \mu I$$

#	Country, Other	Total Cases	New Cases	Total Deaths	New Deaths	Total Recovered	Active Cases	Serious, Critical	Tot Cases/ 1M pop	Deaths/ 1M pop	Total Tests	Tests/ 1M pop	Population
	World	10,711,503	+132,609	516,664	+3,453	5,862,515	4,332,324	57,767	1,374	66.3			
1	USA	2,759,423	+31,570	130,496	+374	1,148,875	1,480,052	15,803	8,337	394	34,519,617	104,288	331,002,277
2	Brazil	1,426,913	+18,428	60,194	+538	790,040	576,679	8,318	6,713	283	3,070,447	14,445	212,558,178
3	Russia	654,405	+6,556	9,536	+216	422,931	221,938	2,300	4,484	65	19,852,167	136,035	145,934,619
4	India	605,216	+19,424	17,848	+438	359,891	227,477	8,944	439	13	8,826,585	6,396	1,379,974,505
5	UK	313,483	+829	43,906	+176	N/A	N/A	238	4,618	647	9,662,051	142,327	67,886,052
6	Spain	296,739	+388	28,363	+8	N/A	N/A	617	6,347	607	5,448,984	116,544	46,754,824
7	Peru	285,213		9,677		174,535	101,001	1,185	8,651	294	1,679,386	50,937	32,969,875
8	Chile	282,043	+2,650	5,753	+65	245,443	30,847	2,106	14,754	301	1,109,792	58,056	19,115,944
9	Italy	240,760	+182	34,788	+21	190,717	15,255	87	3,982	575	5,445,476	90,065	60,461,520
10	Iran	230,211	+2,549	10,958	+141	191,487	27,766	3,081	2,741	130	1,693,242	20,160	83,988,944
11	Mexico	226,089	+5,432	27,769	+648	134,957	63,363	378	1,754	215	581,580	4,511	128,929,303
12	Pakistan	213,470	+4,133	4,395	+91	100,802	108,273	2,741	967	20	1,305,510	5,911	220,861,534
13	Turkey	201,098	+1,192	5,150	+19	175,422	20,526	1,035	2,384	61	3,433,963	40,717	84,336,637
14	Germany	196,296	+464	9,059	+7	179,800	7,437	329	2,343	108	5,873,563	70,103	83,784,248
15	Saudi Arabia	194,225	+3,402	1,698	+49	132,760	59,767	2,272	5,579	49	1,674,487	48,102	34,811,071
16	France	165,719	+918	29,861	+18	76,539	59,319	582	2,539	457	1,384,633	21,213	65,273,746
17	South Africa	159,333	+8,124	2,749	+92	76,025	80,559	539	2,687	46	1,666,939	28,107	59,305,978

Covid-19 dynamics

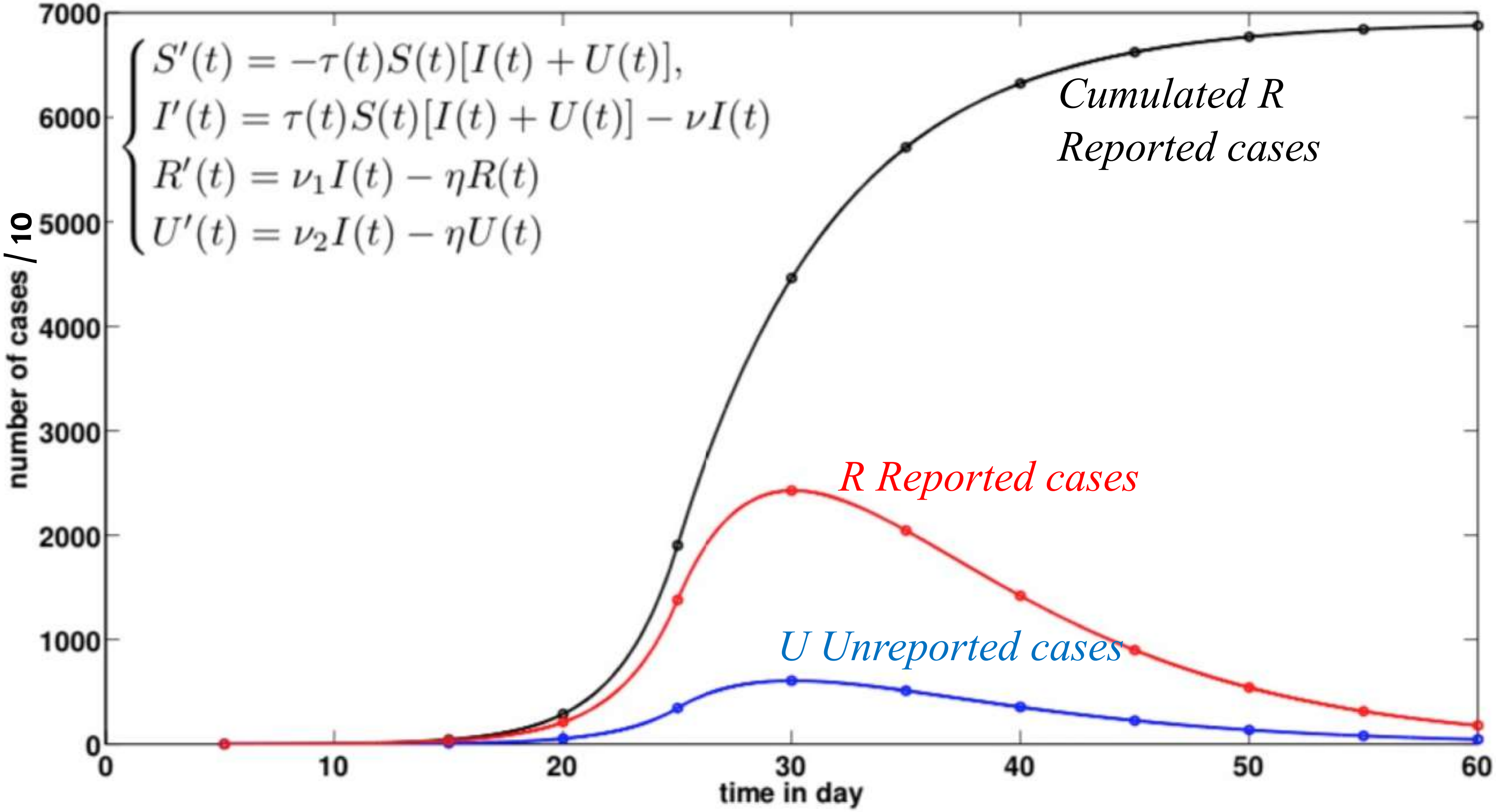

Liu, Z.; Magal, P.; Seydi, O.; Webb, G. Understanding Unreported Cases in the COVID-19 Epidemic Outbreak in Wuhan, China, and the Importance of Major Public Health Interventions. *Biology* 2020, 9, 50.

Linear prediction before and after inflexion

		Before resp. date (sd)		After resp.date (sd)	
Country	Trend change	Linear term	Quad. term	Linear term	Quad. term
Germany	2020-04-04	0.3860(0.0322)	-0.0051(0.0008)	-0.0638(0.0091)	3e-04(4e-04)
French	2020-04-01	0.4094(0.0238)	-0.0054(0.0006)	-0.0508(0.0220)	0(0)
Italy	2020-03-22	0.3410 (0.0205)	-0.0045 (0.0006)	-0.0090 (0.0049)	-5e-04 (2e-04)
Morocco	2020-04-17	0.1882(0.0382)	-0.0018(0.0011)	0.0025 (0.0254)	-6e-04(7e-04)
UK	2020-04-12	0.3403 (0.0169)	-0.0037 (0.0004)	0.0230 (0.0101)	-9e-04 (3e-04)
USA	2020-04-26	0.4489(0.0251)	-0.0048(0.0004)	-0.0092 (0.0217)	1e-04 (8e-04)
Spain	2020-04-01	0.3957(0.0267)	-0.0051(0.0006)	-0.0639 (0.0131)	0 (3e-04)

L. Hobbad, M. Alahiane, M. Rachdi, I. Ouassou, JD

SPAIN

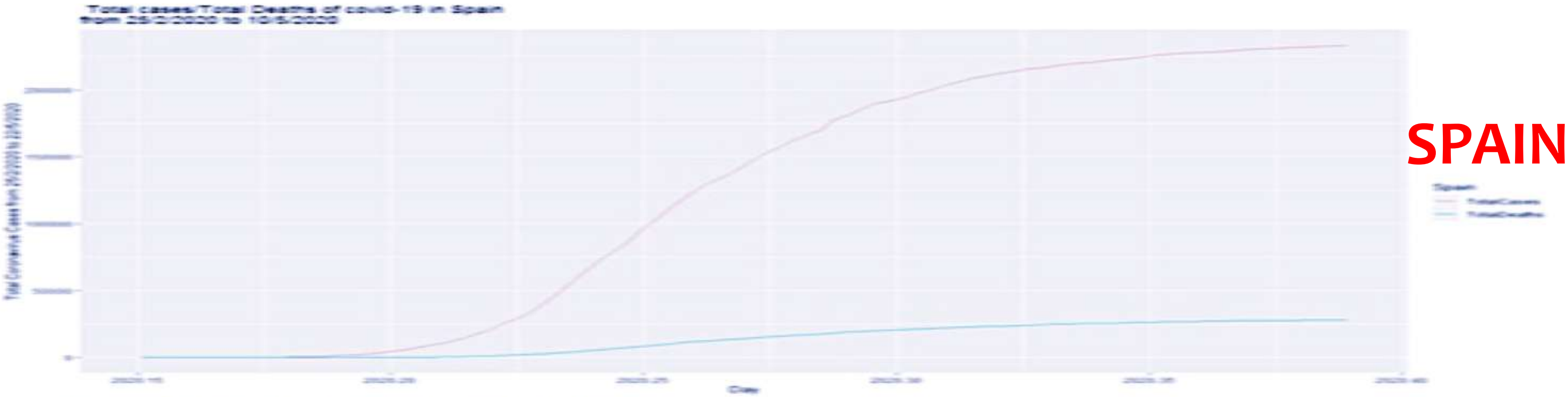

1137, but 510 yesterday !

28/5/2020

FRANCE

Daily New Cases in France form 25/02/2020 to 22/05/2020

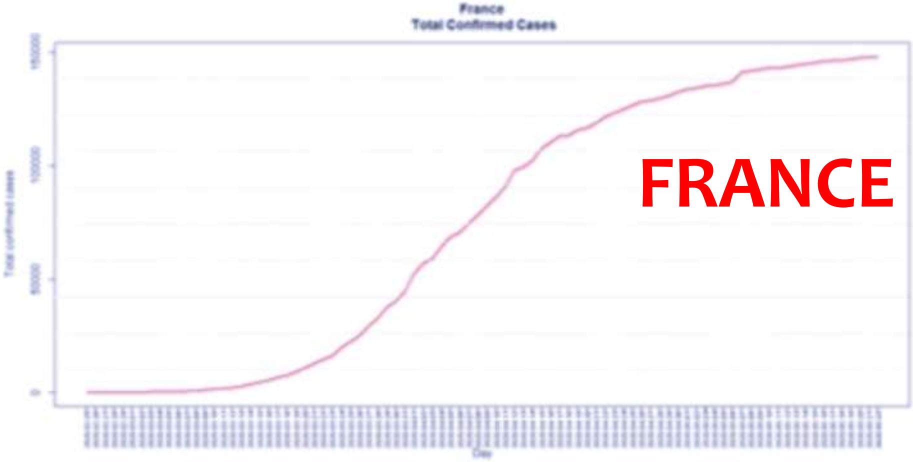

Incidence of Covid-19 in France

log_prevalence of Covid-19 in France

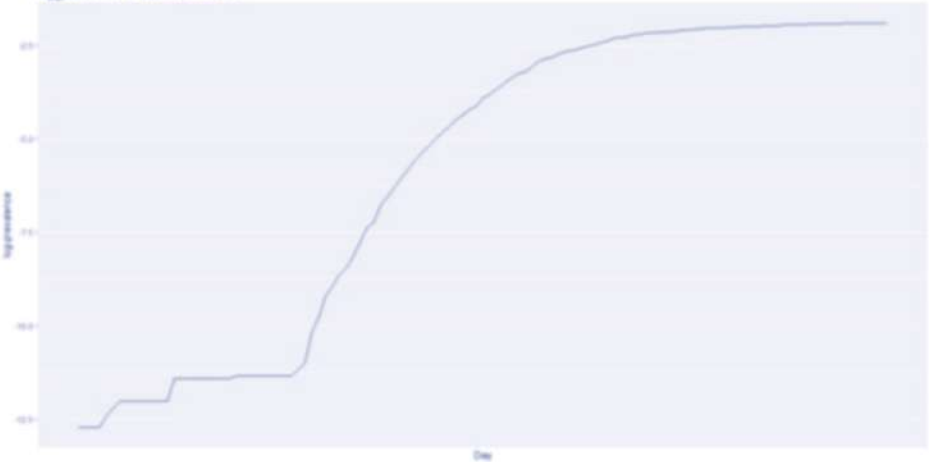

Forecasts from Dynamic regression models

1325, but yesterday 191 !

29/05/2020

Dependence on air ambiant temperature

Mean temperature in France covid-19 spread

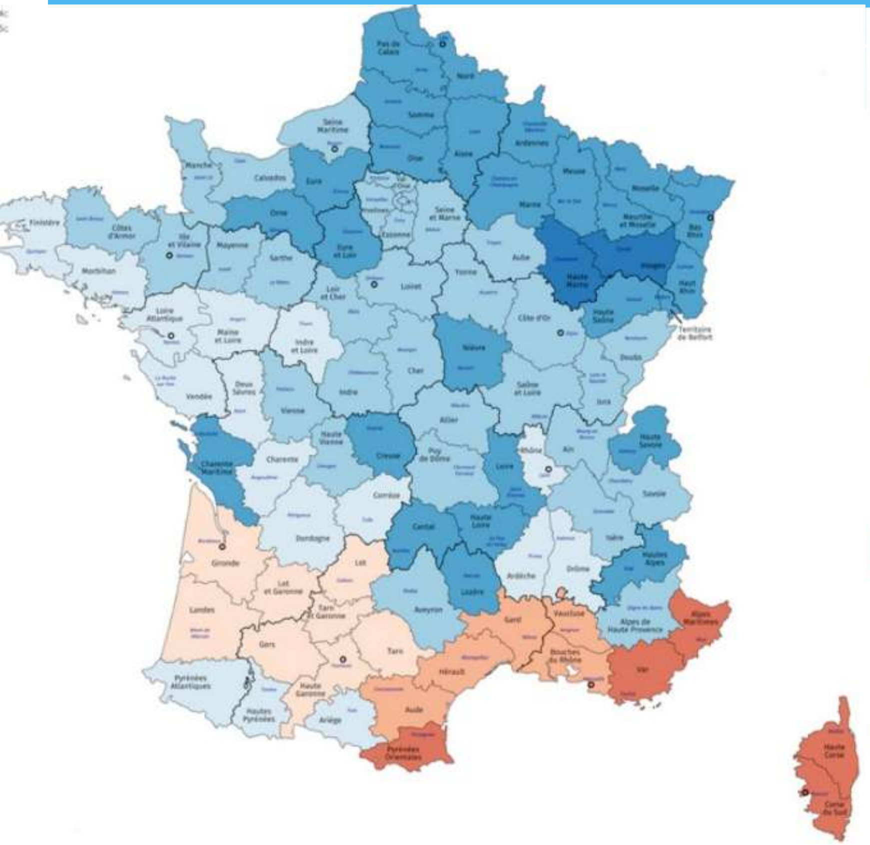

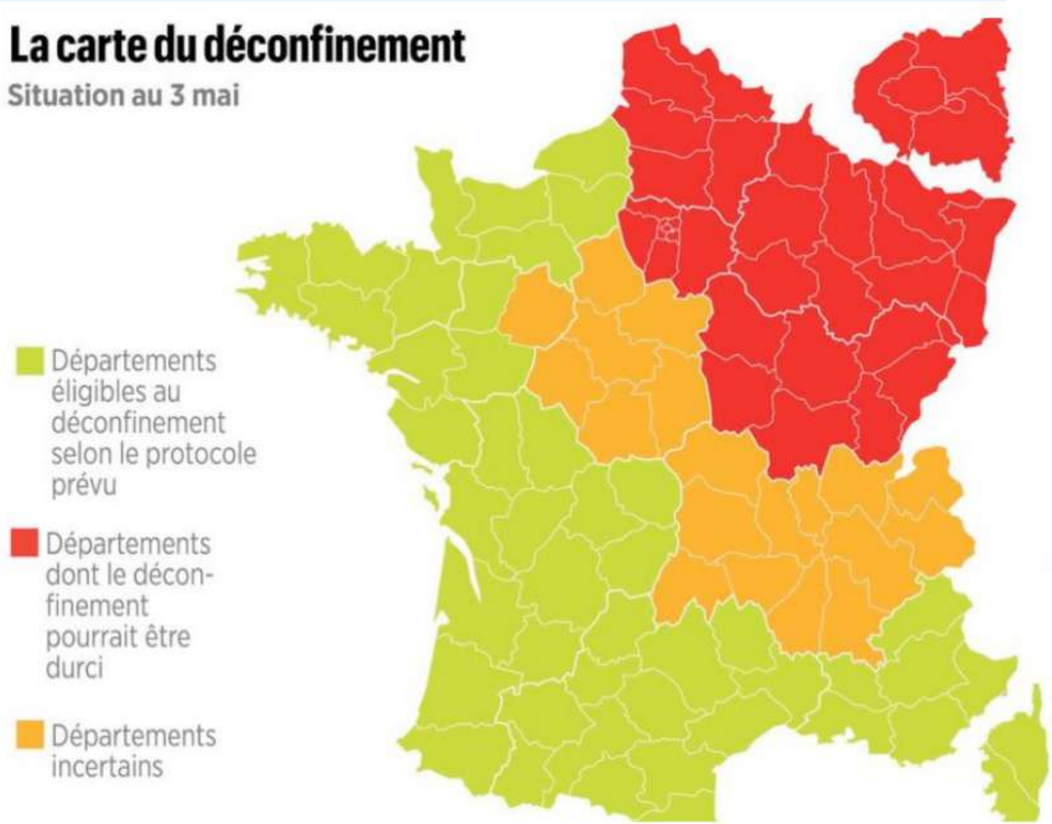

La carte du déconfinement

Situation au 3 mai

🟩 Départements éligibles au déconfinement selon le protocole prévu

🟥 Départements dont le déconfinement pourrait être durci

🟧 Départements incertains

https://www.reddit.com/r/MapPorn/comments/7rq6uh/average_annual_temperature_in_departments_of/

http://www.leparisien.fr/societe/coronavirus-135-deces-en-24-heures-une-nouvelle-carte-de-deconfinement-03-05-2020-8310096.php

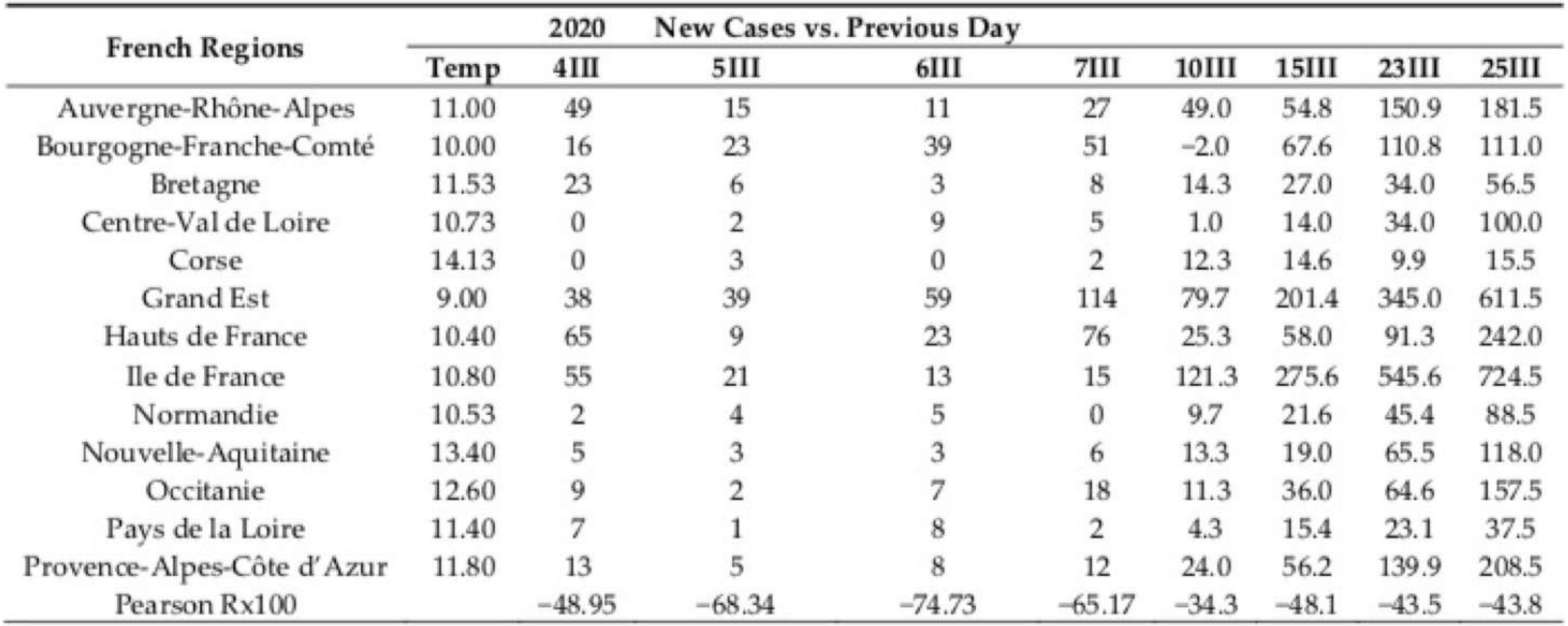

French Regions		2020	New Cases vs. Previous Day						
	Temp	4III	5III	6III	7III	10III	15III	23III	25III
Auvergne-Rhône-Alpes	11.00	49	15	11	27	49.0	54.8	150.9	181.5
Bourgogne-Franche-Comté	10.00	16	23	39	51	−2.0	67.6	110.8	111.0
Bretagne	11.53	23	6	3	8	14.3	27.0	34.0	56.5
Centre-Val de Loire	10.73	0	2	9	5	1.0	14.0	34.0	100.0
Corse	14.13	0	3	0	2	12.3	14.6	9.9	15.5
Grand Est	9.00	38	39	59	114	79.7	201.4	345.0	611.5
Hauts de France	10.40	65	9	23	76	25.3	58.0	91.3	242.0
Ile de France	10.80	55	21	13	15	121.3	275.6	545.6	724.5
Normandie	10.53	2	4	5	0	9.7	21.6	45.4	88.5
Nouvelle-Aquitaine	13.40	5	3	3	6	13.3	19.0	65.5	118.0
Occitanie	12.60	9	2	7	18	11.3	36.0	64.6	157.5
Pays de la Loire	11.40	7	1	8	2	4.3	15.4	23.1	37.5
Provence-Alpes-Côte d'Azur	11.80	13	5	8	12	24.0	56.2	139.9	208.5
Pearson Rx100		−48.95	−68.34	−74.73	−65.17	−34.3	−48.1	−43.5	−43.8

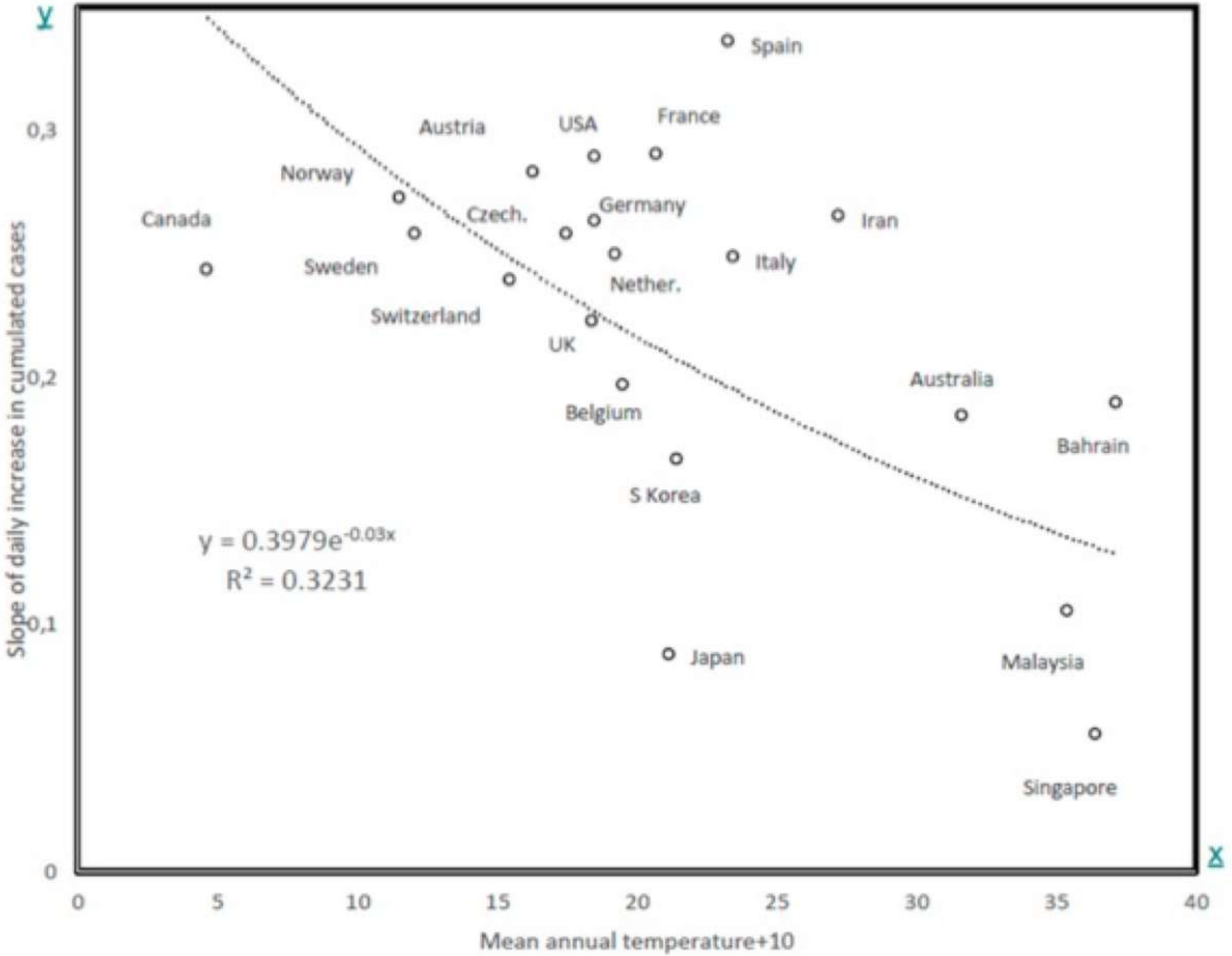

Figure 4. Slope of exponential model fitted to data in Table 3 as a function of mean annual temperature in that country. The Pearson correlation coefficient is R = −0.568, one-tailed *p* = 0.0036.

ARIMA auto-correlation function 1st wave

France

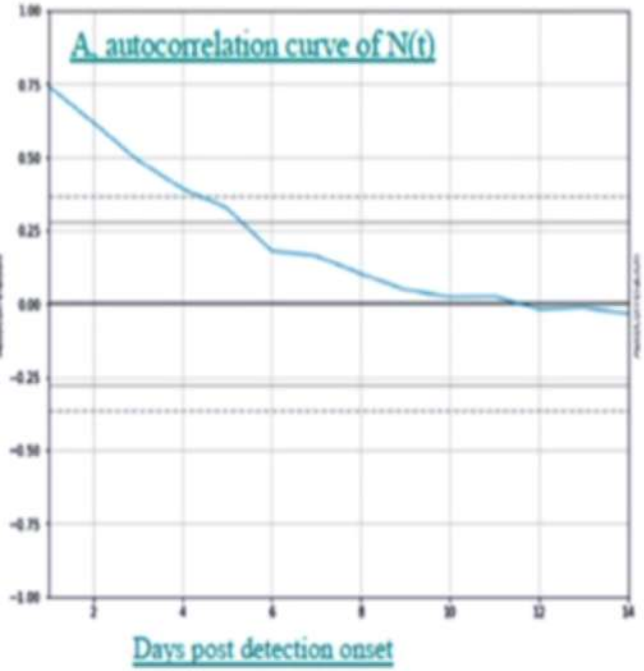

Spain

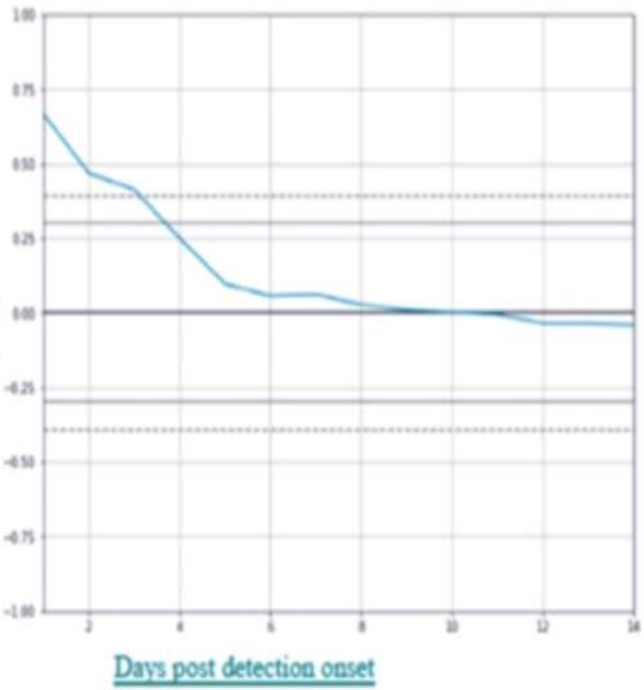

Chile

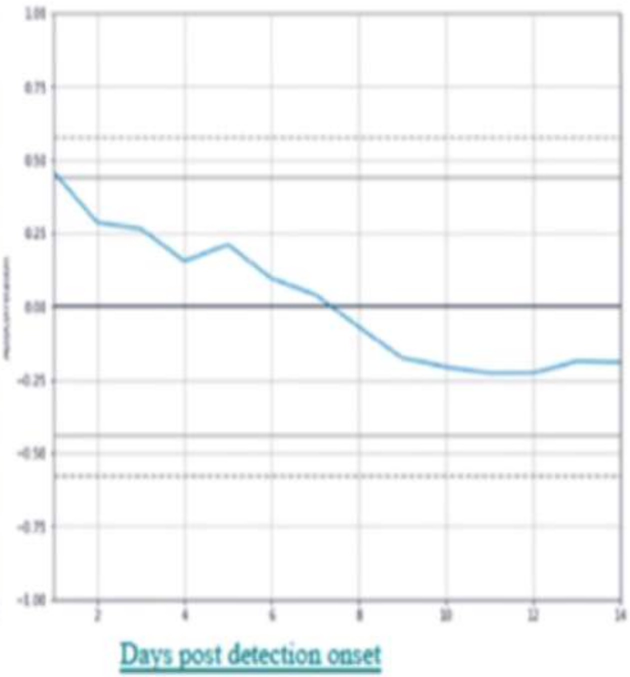

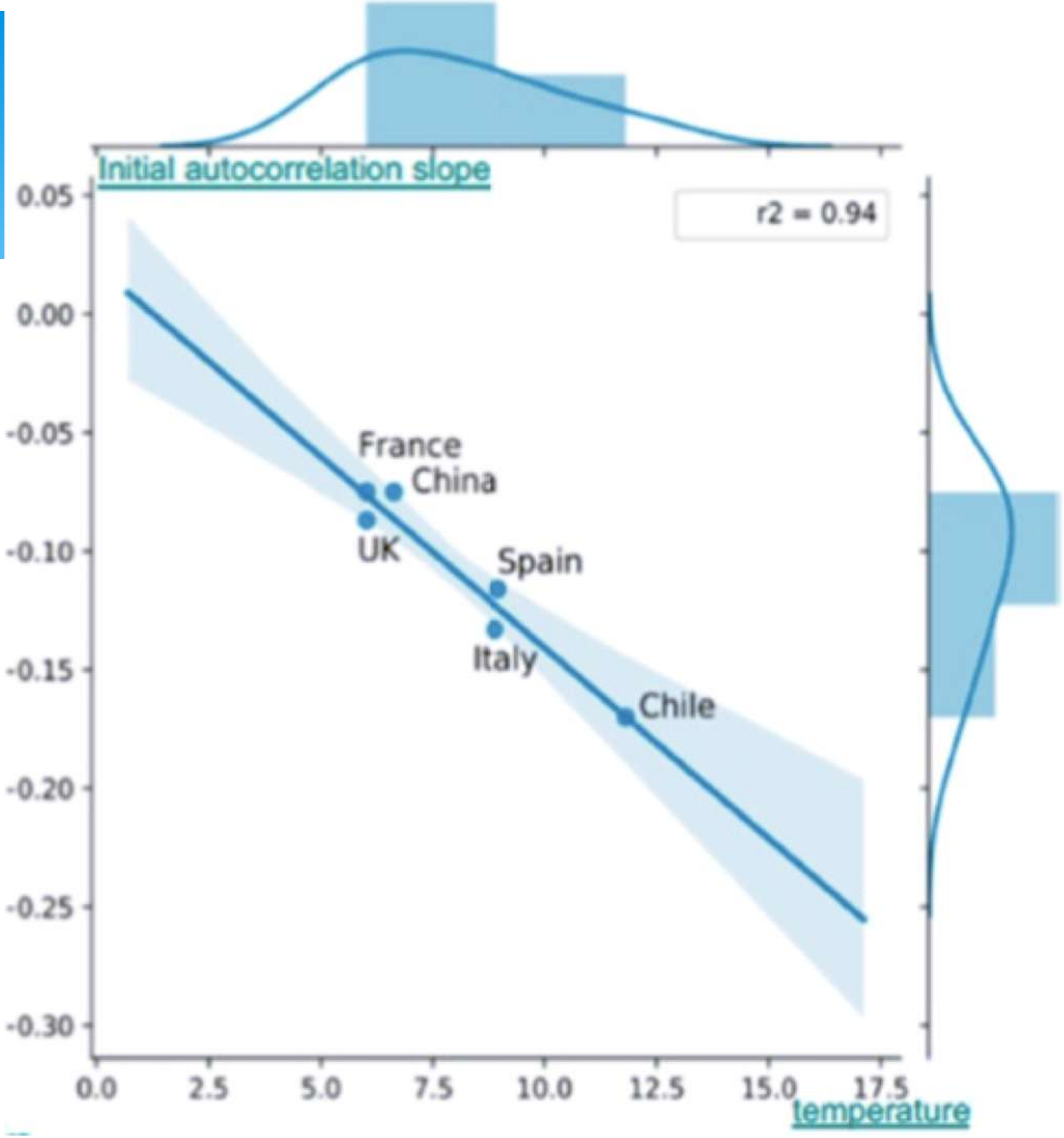
Initial autocorrelation slope
r2 = 0.94
0.05
0.00
-0.05
-0.10
-0.15
-0.20
-0.25
-0.30
France
China
UK
Spain
Italy
Chile
0.0
2.5
5.0
7.5
10.0
12.5
15.0
17.5
temperature

Dependence on genomic factors of the susceptible population

Type II diabetis in France covid-19 spread

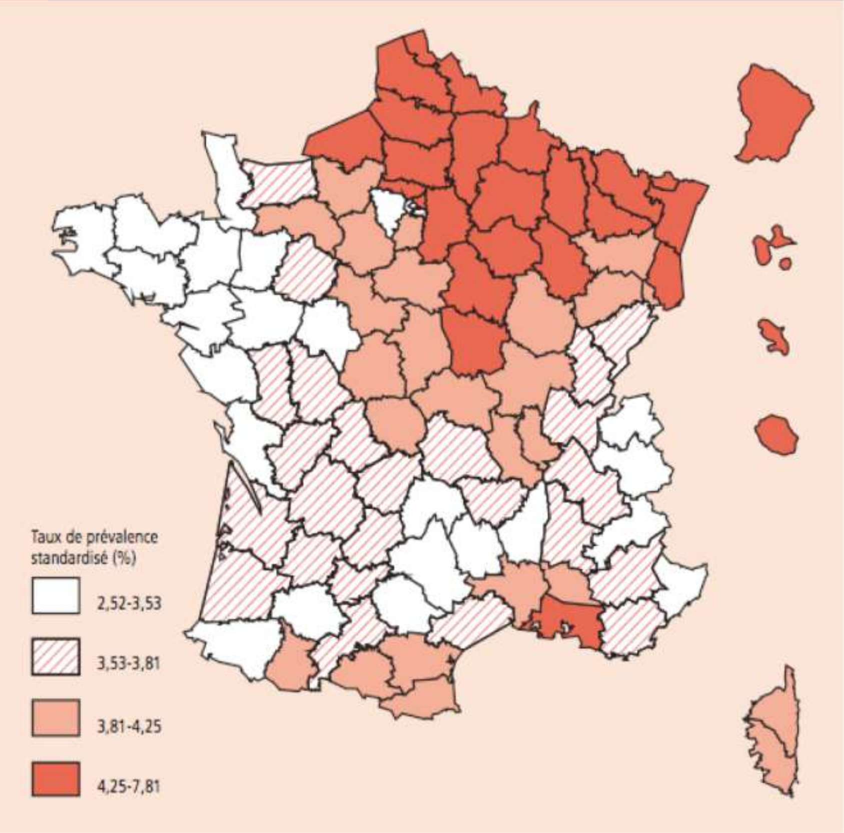

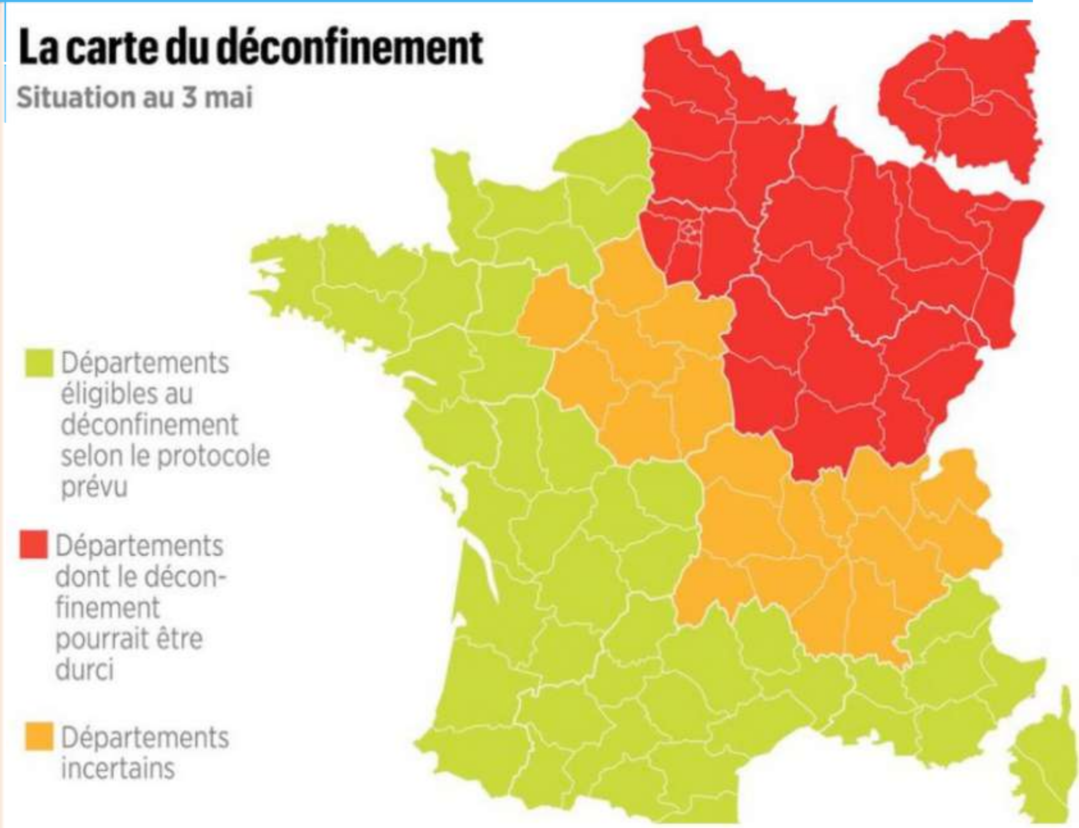
La carte du déconfinement

Situation au 3 mai

Genomic

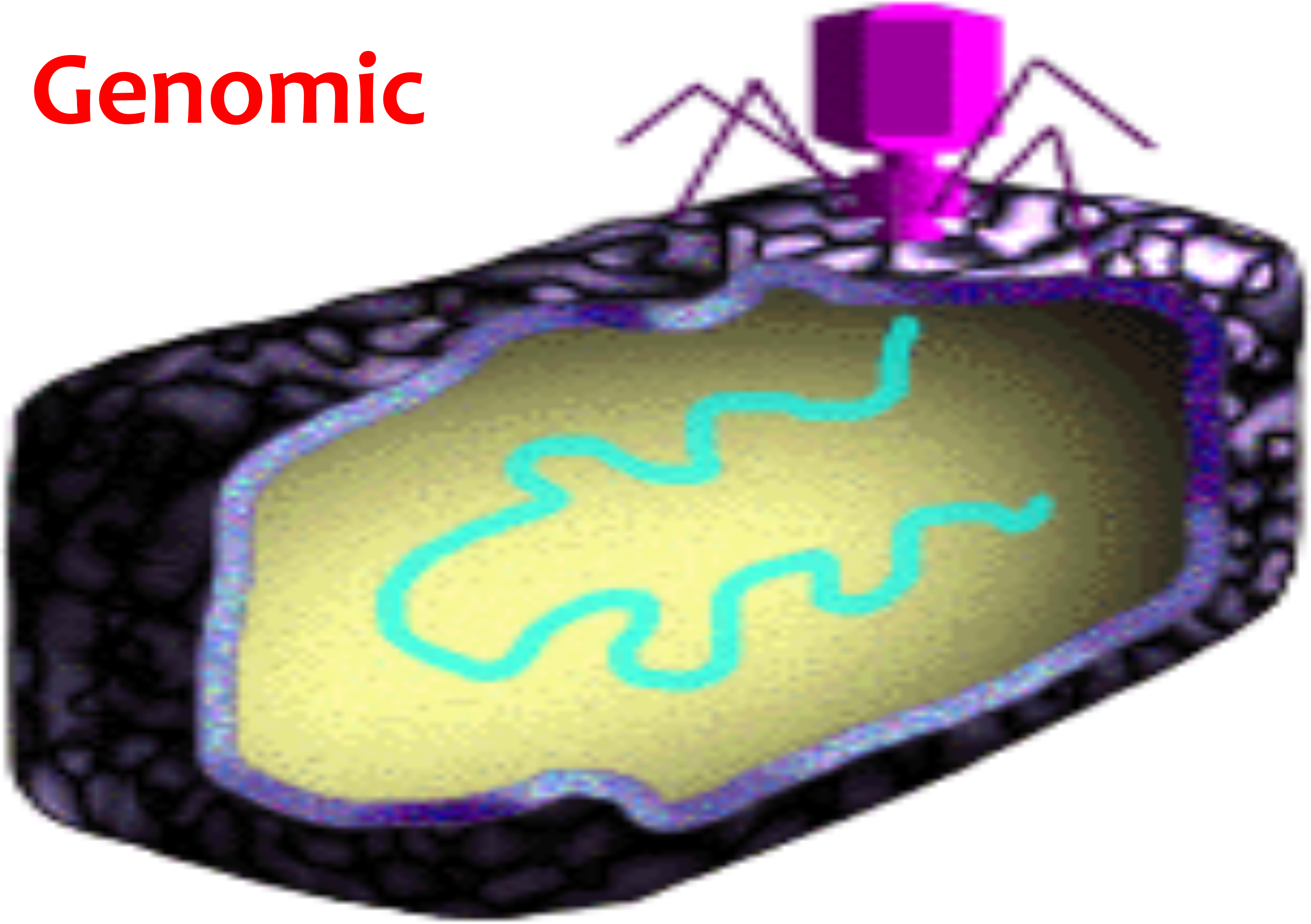

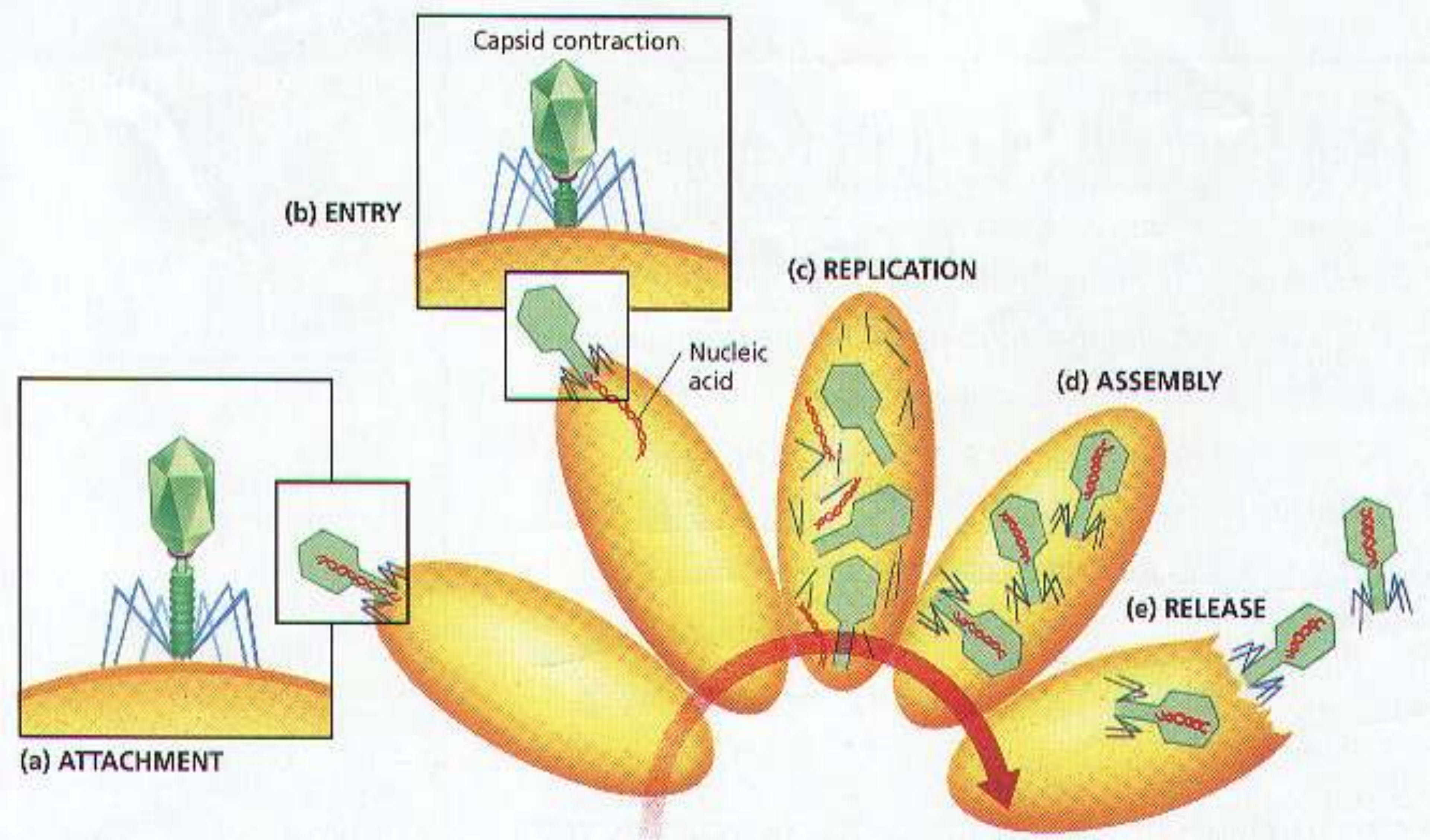
Capsid contraction
(b) ENTRY
(c) REPLICATION
Nucleic acid
(d) ASSEMBLY
(e) RELEASE
(a) ATTACHMENT

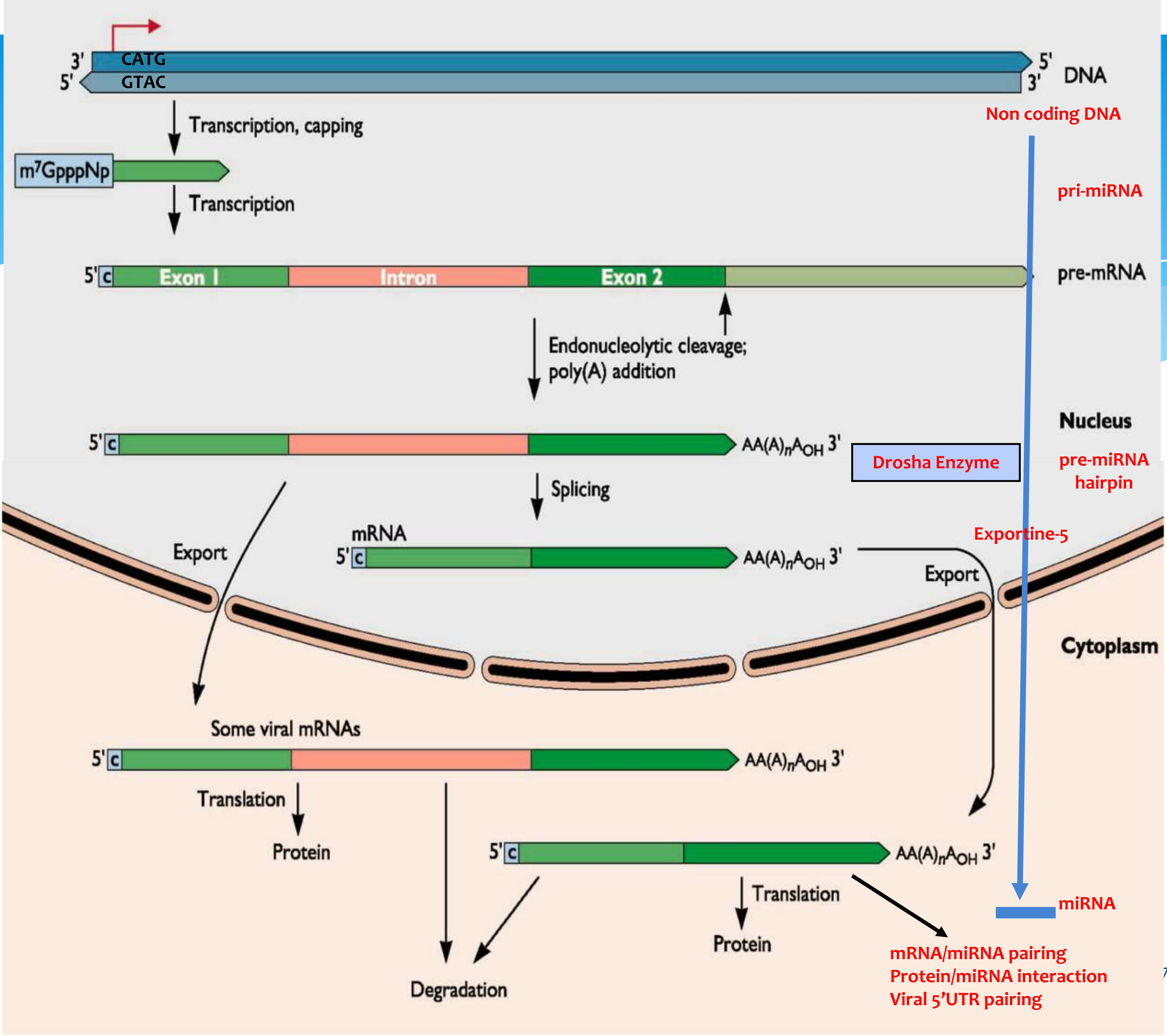

3' CATG 5'

5' GTAC 3'

DNA

Non coding DNA

Transcription, capping

m7GpppNp

Transcription

pri-miRNA

5' C Exon 1 Intron Exon 2

pre-mRNA

Endonucleolytic cleavage;
poly(A) addition

Nucleus

5' C $AA(A)_nA_{OH}$ 3'

Drosha Enzyme

pre-miRNA
hairpin

Splicing

mRNA

5' C $AA(A)_nA_{OH}$ 3'

Export

Exportine-5

Export

Cytoplasm

Some viral mRNAs

5' C $AA(A)_nA_{OH}$ 3'

Translation

Protein

5' C $AA(A)_nA_{OH}$ 3'

Translation

Protein

Degradation

miRNA

mRNA/miRNA pairing
Protein/miRNA interaction
Viral 5'UTR pairing

Generation of retroviral genomic RNA from integrated retroviral DNA

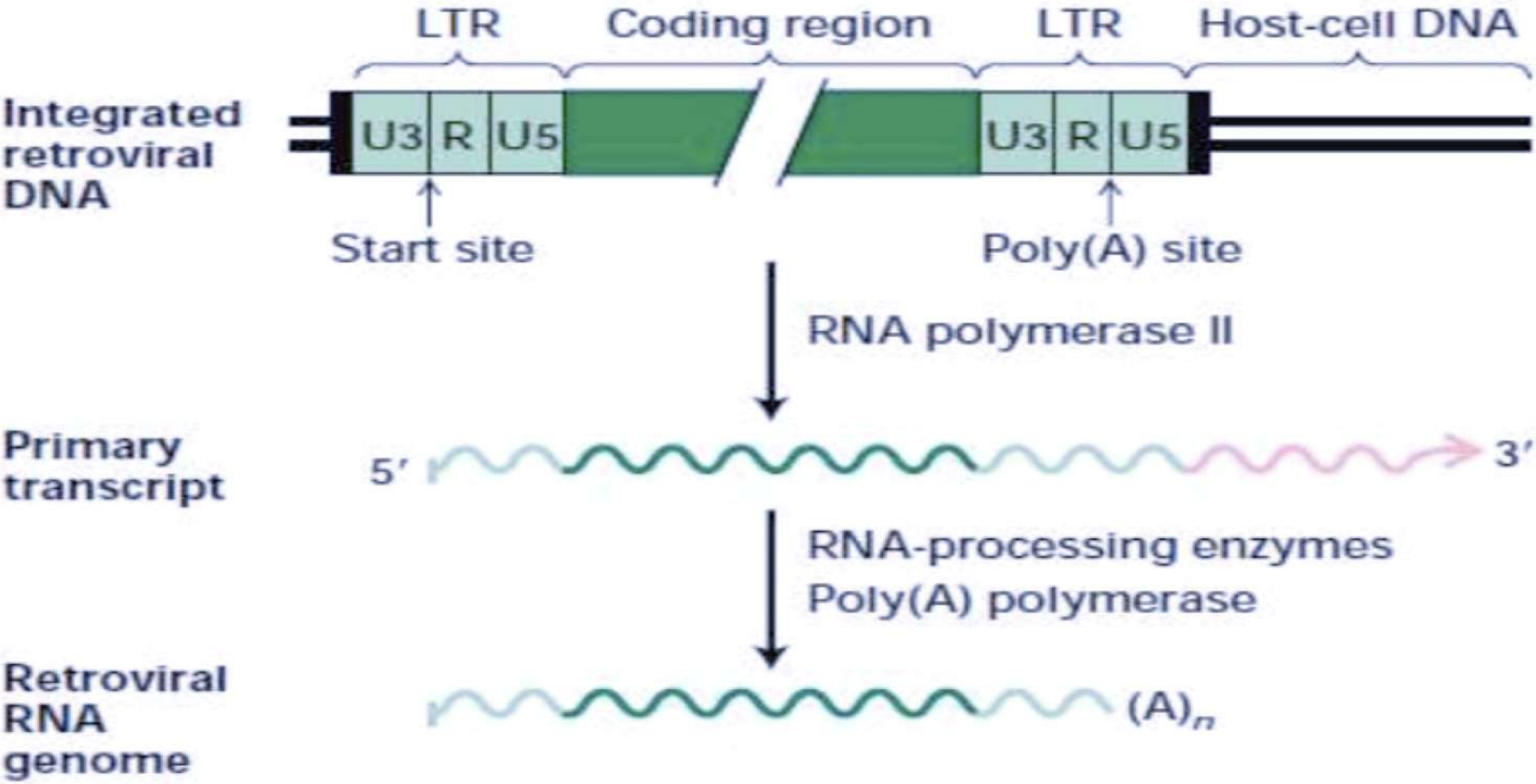

Ref: Molecular cell biology(lodish et all. 2008)

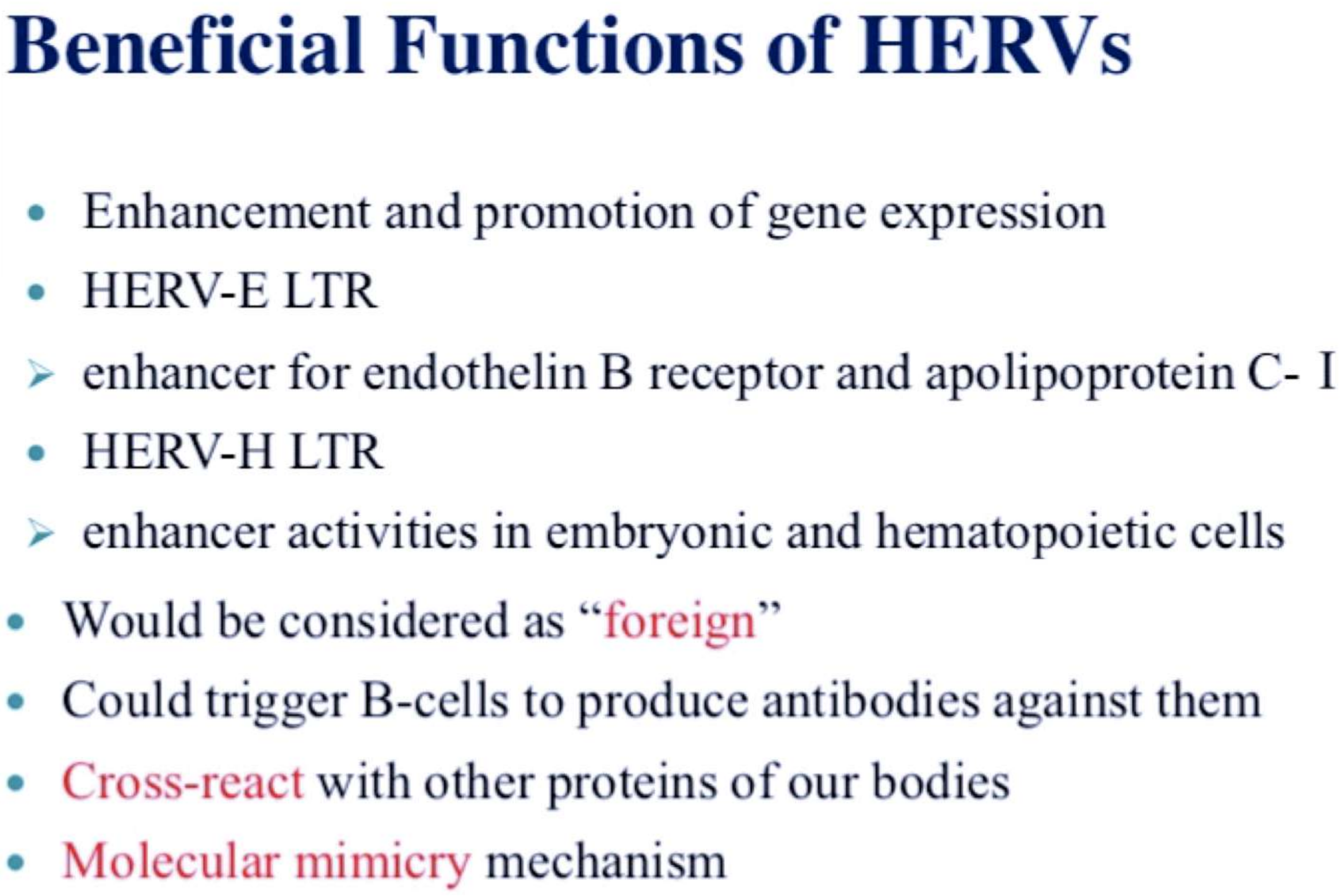

Beneficial Functions of HERVs

- Enhancement and promotion of gene expression
- HERV-E LTR
  - ➢ enhancer for endothelin B receptor and apolipoprotein C- I
- HERV-H LTR
  - ➢ enhancer activities in embryonic and hematopoietic cells
- Would be considered as “foreign”
- Could trigger B-cells to produce antibodies against them
- Cross-react with other proteins of our bodies
- Molecular mimicry mechanism

Homo sapiens endogenous retrovirus HERV-K102, complete sequence GenBank: AF164610.1: 1112-2596 Gag protein

ATGGGGCAAACTAAAAGTAAAATTAAAAGTAAATATGCCTCTTATCTCAGCTTTATTAAAATTCTTTTAA
AAAGAGGGGAGTTAAAGTATCTACAAAAAATCTAA**TCAAG**CTAT**TTCAA**ATAATAGAACAATTTTGCCC
ATGGTTTCCAGAACAAGGAACTTTAGATCTAA**AAGAT**TGGAAAAGAAT**TGGTA**AGGAACTAAAACAAGCA
GGTAGGAAGGGTAATAT**CATTCCACTT**ACAGTATG**GAATG**ATTGG**GCCATT**ATTAAAGCA**GCTTTAGAAC**
CATTTCAAACAGAAG**AAGAT**AGCGTTTCAGTTTCTGATGCCCTTGGAAGCTGTATAATAGATTGTA**ATGA**
AAACACAAGGAAAAAATCCCAGAAAGAAACGGAAGGTTTACATTGCGAATATGTAGCAGAGCCGGT**AATG**
GCTCAGTCAACGCAAAATGTTGACTATAATCAATTACAGGAGGTGATATATCCTGAAACGTTAAAATTAG
AAGGAAAAGGTCCAGAATTAGTGGG**GCCAT**CAGAGTCTAAACCACGAGGCACAAGTCATCTTCCAGCAGG
TCAGGTGCCCGTAACATTACAACCTCAAAAGCAGGTTAAAGAAAATAAGACCCAACCGCCAGTAGCCTAT
CAA**TACTG**GCCTCCGGCTGAACTTCAGTATCGGCCACCCCCAGAAAGTCAGTATGGATATCCAG**GAATG**C
CCCCAGCACCACAGGGCAGGGC**GCCAT**ACCCTCAGCCGCCCACTAGGAGACTTAATCCTACGGCACCACC
TAGTAGACAGGGTAG**TGAAT**TAC**ATGAA**ATTATTGATAAA**TCAAGA**AAGGAAGGAGA**TACTG**AGGCATGG
CAATTCCCAGTAACGTTAGAACCGA**TGCCA**CCTGGAGAAGGAGCC**CAAGA**GGGAGAGCCTCCCACAGTTG
AGGCCAGATACAAGTCTTTTTCGATAAAAATGCTAA**AAGATATGAA**AGAGGGAGTAAAACAGTATGGACC
CAACTCCCCTTATATGAGGACATTATTAGATT**CCATT**GCTCATGGACATAGACT**CATTC**CTTATGATTGG
GAGATTCTGGCAAAATCGTCTCTCTCACCCTCTCAATTTTTACAATTTAAGACTTGGTGGATTGATGG**GG**
TACAAGAACAGGTCCGAAGAAATAGGG**CTGCCA**ATCCTCCAGTTAACAT**AGATG**CAGATCAACTATTAGG
AATAGGTCAAAATTGGA**GTACT**ATTAGTCAACAAGCATTAATGCAAAATGAG**GCCATT**GAGCAAGTTAGA
GCTAT**CTGCC**TTAGAGCCTGGGAAAAAATC**CAAGA**CCCAGGAAGTAC**CTGCC**CCTCATTTAATACAGTAA
GACAAGG**TTCAA**AAGAGCCCTATCCTGATTTTGTGGCAAGGCTC**CAAGATG**TTGCTCAAAAGTCAATTGC
C**GATGAA**AAAGCCCGTAAGGTCATAGTGGAGTTGATGGCAT**ATGAA**AACGCCAATCCTGATGTCAATCA**G**
CCATTAA**GCCATT**AA

Observed 50 ancient pentamers (red) among 1481 possible = 3.4% (expected 2.1%±0.5%)

Figure 5. Complete RNA sequence of the Gag protein of the virus HERV-K102 [36]. The green subsequence of length 14 (271-285) is present in the RNA sequence of the protein S of the virus Covid-19 [22]. Red: pentamers belonging to ancient circular RNAs as measure of the genomic structure's age in evolution [7,8].

Covid-19 protein S gene Furin splicing site

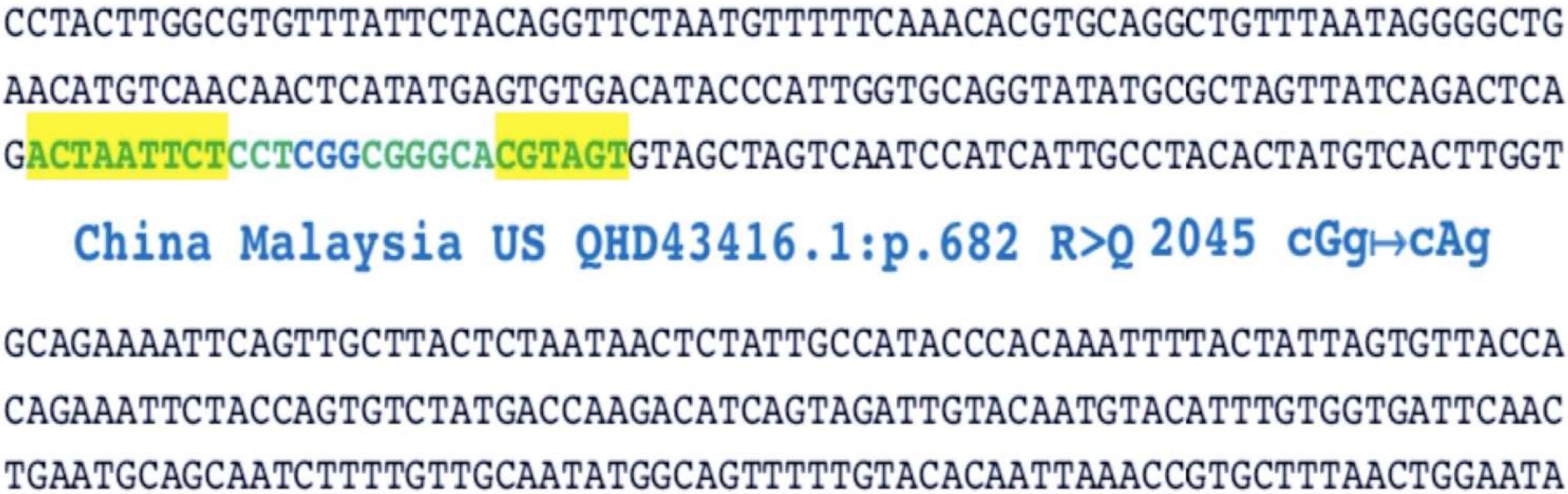

CCTACTTGGCGTGTTTATTCTACAGGTTCTAATGTTTTTCAAACACGTGCAGGCTGTTTAATAGGGGCTG
AACATGTCAACAACTCATATGAGTGTGACATACCCATTGGTGCAGGTATATGCGCTAGTTATCAGACTCA
GACTAATTCTCCTCGGCGGGCACGTAGTGTAGCTAGTCAATCCATCATTGCCTACACTATGTCACTTGGT

China Malaysia US QHD43416.1:p.682 R>Q 2045 cGg↦cAg

GCAGAAAATTCAGTTGCTTACTCTAATAACTCTATTGCCATACCCACAAATTTTACTATTAGTGTTACCA
CAGAAATTCTACCAGTGTCTATGACCAAGACATCAGTAGATTGTACAATGTACATTTGTGGTGATTCAAC
TGAATGCAGCAATCTTTTGTTGCAATATGGCAGTTTTTGTACACAATTAAACCGTGCTTTAACTGGAATA

Covid-19 dynamics depends on genomic factors like retro-viruses

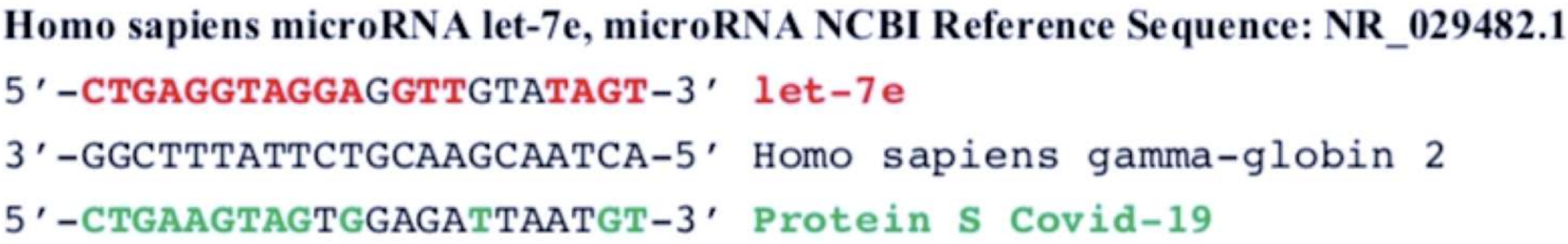

Homo sapiens microRNA let-7e, microRNA NCBI Reference Sequence: NR_029482.1

5′-CTGAGGTAGGAGGTTGTATAGT-3′ let-7e

3′-GGCTTTATTCTGCAAGCAATCA-5′ Homo sapiens gamma-globin 2

5′-CTGAAGTAGTGGAGATTAATGT-3′ Protein S Covid-19

J. Demongeot, E. Drouet, A. Moreira, Y. Rechoum & S. Sené. Micro-RNAs: viral genome and robustness of the genes expression in host. *Phil. Trans. Royal Soc. A*, **367**, 4941-4965 (2009).
J. Demongeot & H. Seligmann. Covid-19 and miRNA-like inhibition power. *Biology* (submitted).

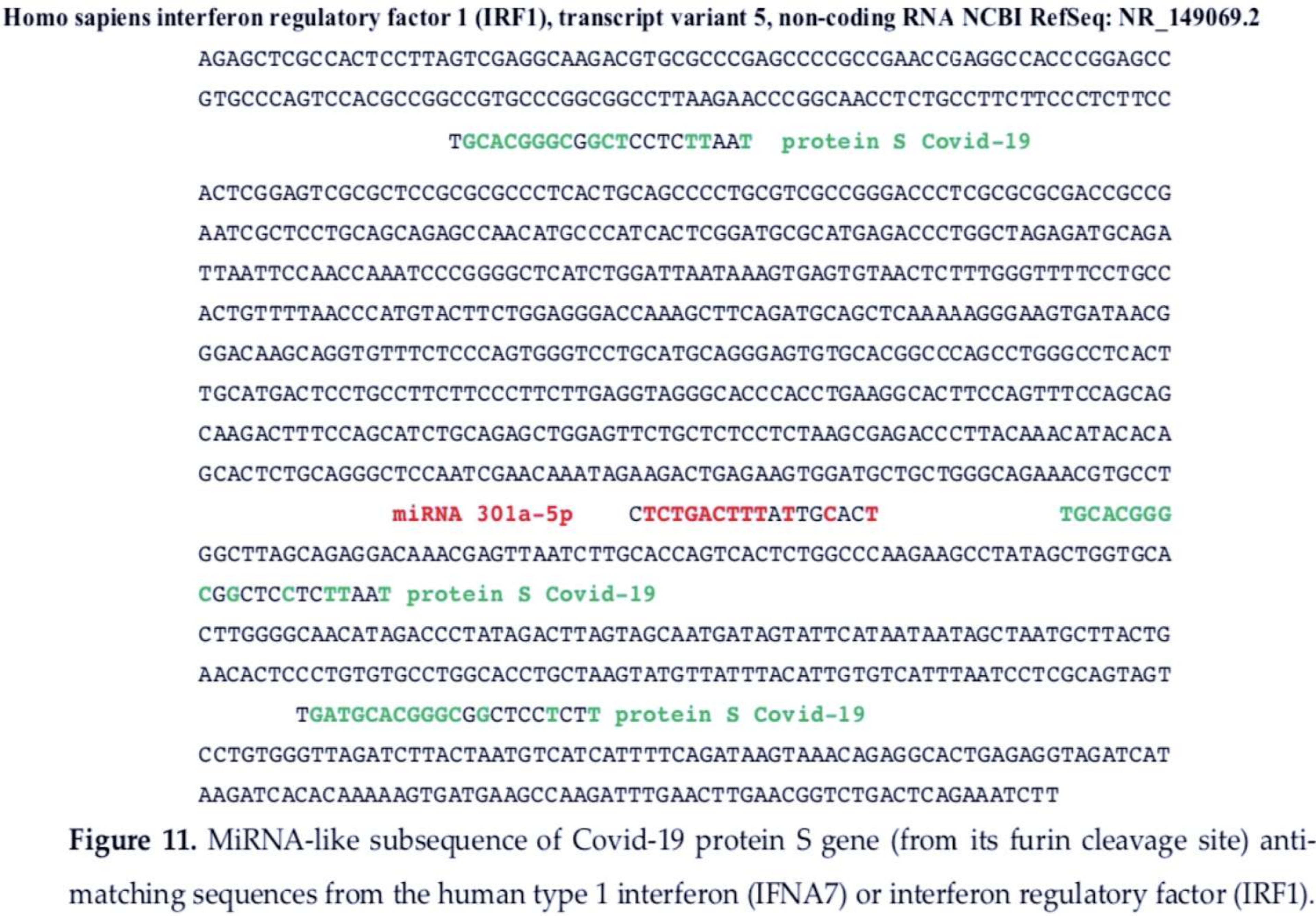

Homo sapiens interferon regulatory factor 1 (IRF1), transcript variant 5, non-coding RNA NCBI RefSeq: NR_149069.2

```
AGAGCTCGCCACTCCTTAGTCGAGGCAAGACGTGCGCCCGAGCCCCGCCGAACCGAGGCCACCCGGAGCC
GTGCCCAGTCCACGCCGGCCGTGCCCGGCGGCCTTAAGAACCCGGCAACCTCTGCCTTCTTCCCTCTTCC
                  TGCACGGGCGGCTCCTCTTAAT  protein S Covid-19
ACTCGGAGTCGCGCTCCGCGCGCCCTCACTGCAGCCCCTGCGTCGCCGGGACCCTCGCGCGACCGCCG
AATCGCTCCTGCAGCAGAGCCAACATGCCCATCACTCGGATGCGCATGAGACCCTGGCTAGAGATGCAGA
TTAATTCCAACCAAATCCCGGGGCTCATCTGGATTAATAAAGTGAGTGTAACTCTTTGGGTTTTCCTGCC
ACTGTTTTAACCCATGTACTTCTGGAGGGACCAAAGCTTCAGATGCAGCTCAAAAAGGGAAGTGATAACG
GGACAAGCAGGTGTTTCTCCCAGTGGGTCCTGCATGCAGGGAGTGTGCACGGCCCAGCCTGGGCCTCACT
TGCATGACTCCTGCCTTCTTCCCTTCTTGAGGTAGGGCACCCACCTGAAGGCACTTCCAGTTTCCAGCAG
CAAGACTTTCCAGCATCTGCAGAGCTGGAGTTCTGCTCTCCTCTAAGCGAGACCCTTACAAACATACACA
GCACTCTGCAGGGCTCCAATCGAACAAATAGAAGACTGAGAAGTGGATGCTGCTGGGCAGAAACGTGCCT
             miRNA 301a-5p    CTCTGACTTTATTGCACT                  TGCACGGG
GGCTTAGCAGAGGACAAACGAGTTAATCTTGCACCAGTCACTCTGGCCCAAGAAGCCTATAGCTGGTGCA
CGGCTCCTCTTAAT protein S Covid-19
CTTGGGGCAACATAGACCCTATAGACTTAGTAGCAATGATAGTATTCATAATAATAGCTAATGCTTACTG
AACACTCCCTGTGTGCCTGGCACCTGCTAAGTATGTTATTTACATTGTGTCATTTAATCCTCGCAGTAGT
      TGATGCACGGGCGGCTCCTCTT protein S Covid-19
CCTGTGGGTTAGATCTTACTAATGTCATCATTTTCAGATAAGTAAACAGAGGCACTGAGAGGTAGATCAT
AAGATCACACAAAAAGTGATGAAGCCAAGATTTGAACTTGAACGGTCTGACTCAGAAATCTT
```

Figure 11. MiRNA-like subsequence of Covid-19 protein S gene (from its furin cleavage site) anti-matching sequences from the human type 1 interferon (IFNA7) or interferon regulatory factor (IRF1).

Homo sapiens olfactory receptor family 4 subfamily E member 1 (OR4E1), mRNA NCBI Reference Sequence: NM_001317107.1

TTAAATGACCAAATGATTGATGCAGATACTGTGTTATATTAGACTTTTTTTCTAATTCTTTACAGGTTGT
CTAACAAAGAGAATGGAAGAGGCCATCCTACTCAATCAAACTTCTTTAGTGACATATTTTCGGCTTAGAG
GTTTATCTGTAAATCATAAGGCACGGATAGCTATGTTTTCCATGTTCCTCATTTTTTATGTCCTGACACT
GATTGGGAATGTTCTCATTGTCATAACTATTATCTATGACCACCGGCTCCATACTCCCATGTATTTCTTC
CTCAGCAACCTGTCCTTTATTGATGTCTGCCACTCCACTGTCACTGTCCCCAAGATGCTGAGAGACGTGT
GGTCAGAGGAAAAGCTCATCTCTTTTGATGCCTGTGTGACCCAGATGTTCTTCCTGCACCTCTTTGCCTG
CACAGAGATCTTCCTCCTCACCGTCATGGCCTATGATCGGTATGTGGCCATCTGTAAACCCCTGCAGTAC
ATGATAGTGATGAACTGGAAGGTATGTGTGCTGCTGGCTGTGGCCCTCTGGACAGGAGGGACCATCCACT
CCATAGCCCTCACCTCCCTTACCATCAAGCTGCCCTACTGTGGTCCTGATGAGATTGACAACTTCTTCTG
TGATGTACCTCAGGTGATCAAGCTGGCCTGCATTGACACCCACGTCATTGAGATCCTCATTGTCTCCAAC
AGTGGATTGATCTCCGTGGTCTGTTTTGTGGTCCTGGTGGTGTCCTACGCAGTCATCCTGGTGAGTCTGA
GGCAGCAGATCTCCAAGGGCAAGCGGAAGGCCCTGTCCACCTGTGCAGCCCATCTCACTGTAGTTACACT
ATCGATGTGA
GTTCCTGGGACACTGCATCTTCATCTATTCCCGCCCATCCACCAGCCTCCCAGAGGACAAGGTAGTATCT
TGCACGGGCGG
GTGTTTTTCACTGCAGTCACCCCCCTGCTGAACCCCATTATCTATACCCTTAGGAATGAAGAAATGAAGA
GTGCCTTAAACAAGTTAGTGGGAGAAAAGAGAGAAAAGAAGAAAAATGAAAATGTCTACGTCCTTAGGA
TACGTGGTGCTCCAAATTAAAGAAGCGCCTTGCAAAGAATAAGTTACATACCATAT

Figure 9. Complete mRNA sequence of the human olfactory receptor family 4 subfamily E member 1 (OR4E1) [22]. The RNA sequence in green is a sub-sequence of the protein S of Covid-19, which can exert a miRNA-like inhibition of the translation of OR4E1. The probability to observe such an anti-match of length 12 by chance in a sequence of 577 nucleotides equals 5 10^{-4}.

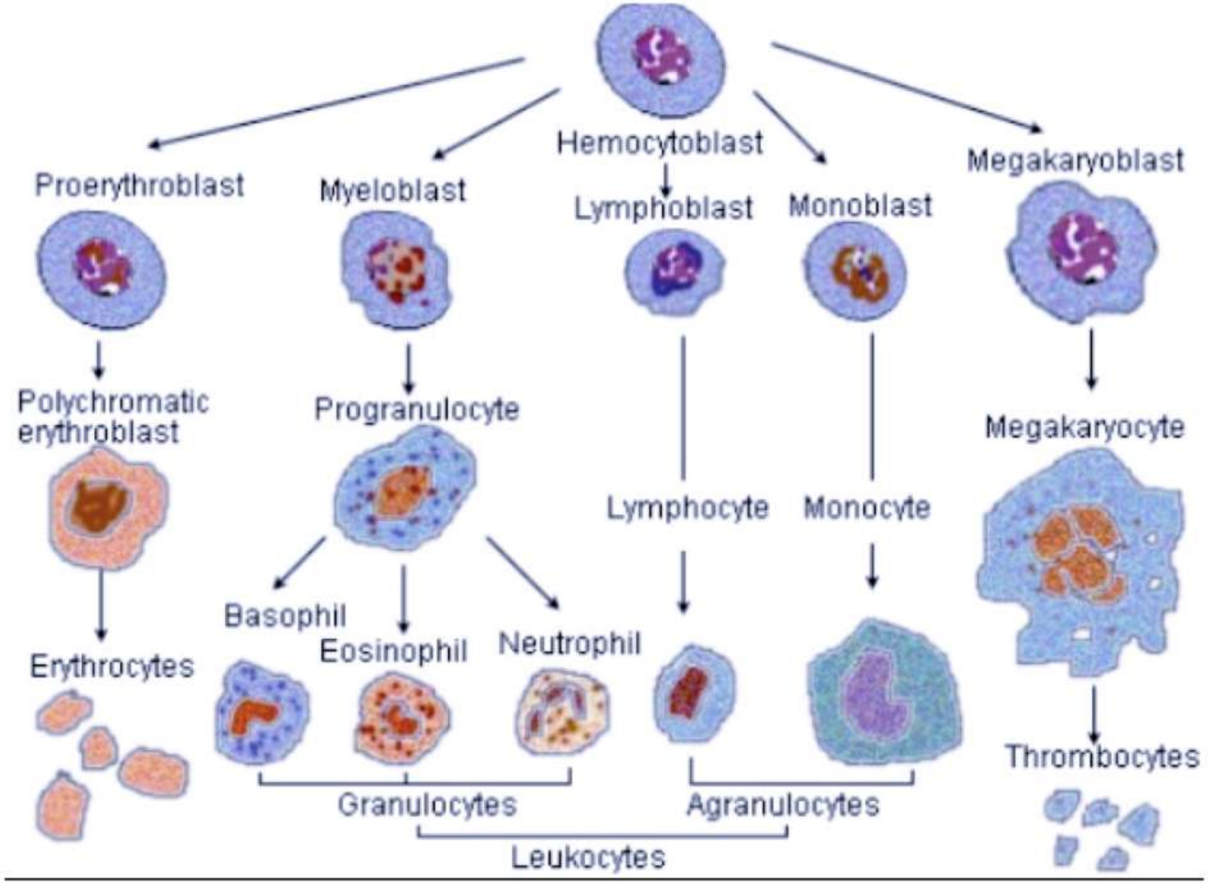

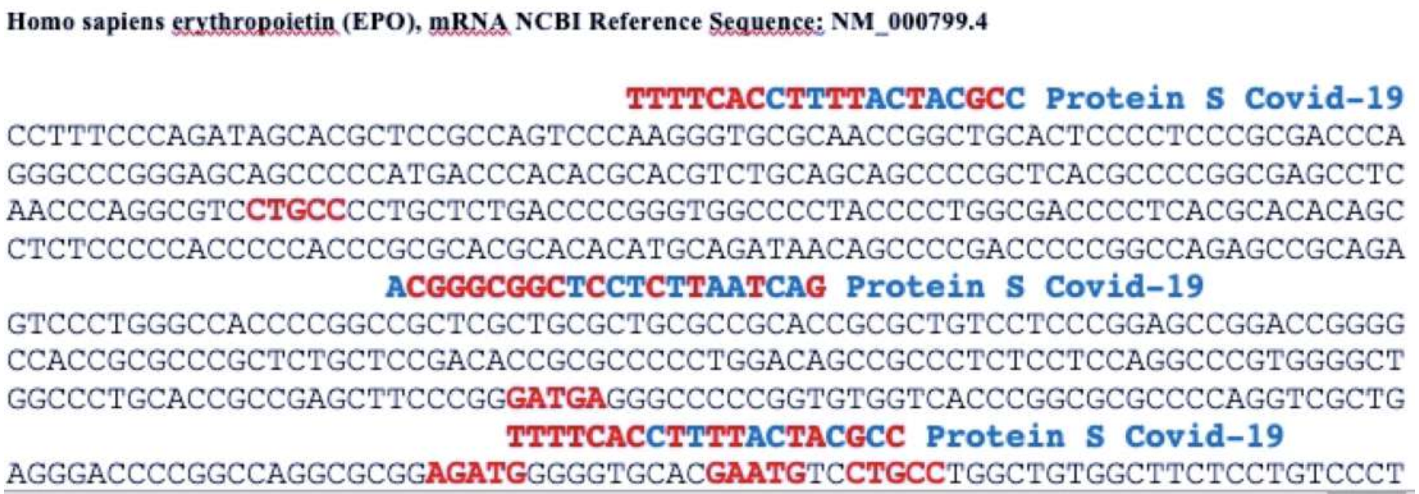

Homo sapiens erythropoietin (EPO), mRNA NCBI Reference Sequence: NM_000799.4

```
                                 TTTTCACCTTTTACTACGCC Protein S Covid-19
CCTTTCCCAGATAGCACGCTCCGCCAGTCCCAAGGGTGCGCAACCGGCTGCACTCCCCTCCCGCGACCCA
GGGCCCGGGAGCAGCCCCCATGACCCACACGCACGTCTGCAGCAGCCCCGCTCACGCCCCGGCGAGCCTC
AACCCAGGCGTCCTGCCCCTGCTCTGACCCCGGGTGGCCCCTACCCCTGGCGACCCCTCACGCACACAGC
CTCTCCCCCACCCCCACCCGCGCACGCACACATGCAGATAACAGCCCCGACCCCCGGCCAGAGCCGCAGA
                    ACGGGCGGCTCCTCTTAATCAG Protein S Covid-19
GTCCCTGGGCCACCCCGGCCGCTCGCTGCGCTGCGCCGCACCGCGCTGTCCTCCCGGAGCCGGACCGGGG
CCACCGCGCCCGCTCTGCTCCGACACCGCGCCCCCTGGACAGCCGCCCTCTCCTCCAGGCCCGTGGGGCT
GGCCCTGCACCGCCGAGCTTCCCGGGATGAGGGCCCCCGGTGTGGTCACCCGGCGCGCCCCAGGTCGCTG
                          TTTTCACCTTTTACTACGCC Protein S Covid-19
AGGGACCCCGGCCAGGCGCGGAGATGGGGGTGCACGAATGTCCTGCCTGGCTGTGGCTTCTCCTGTCCCT
```

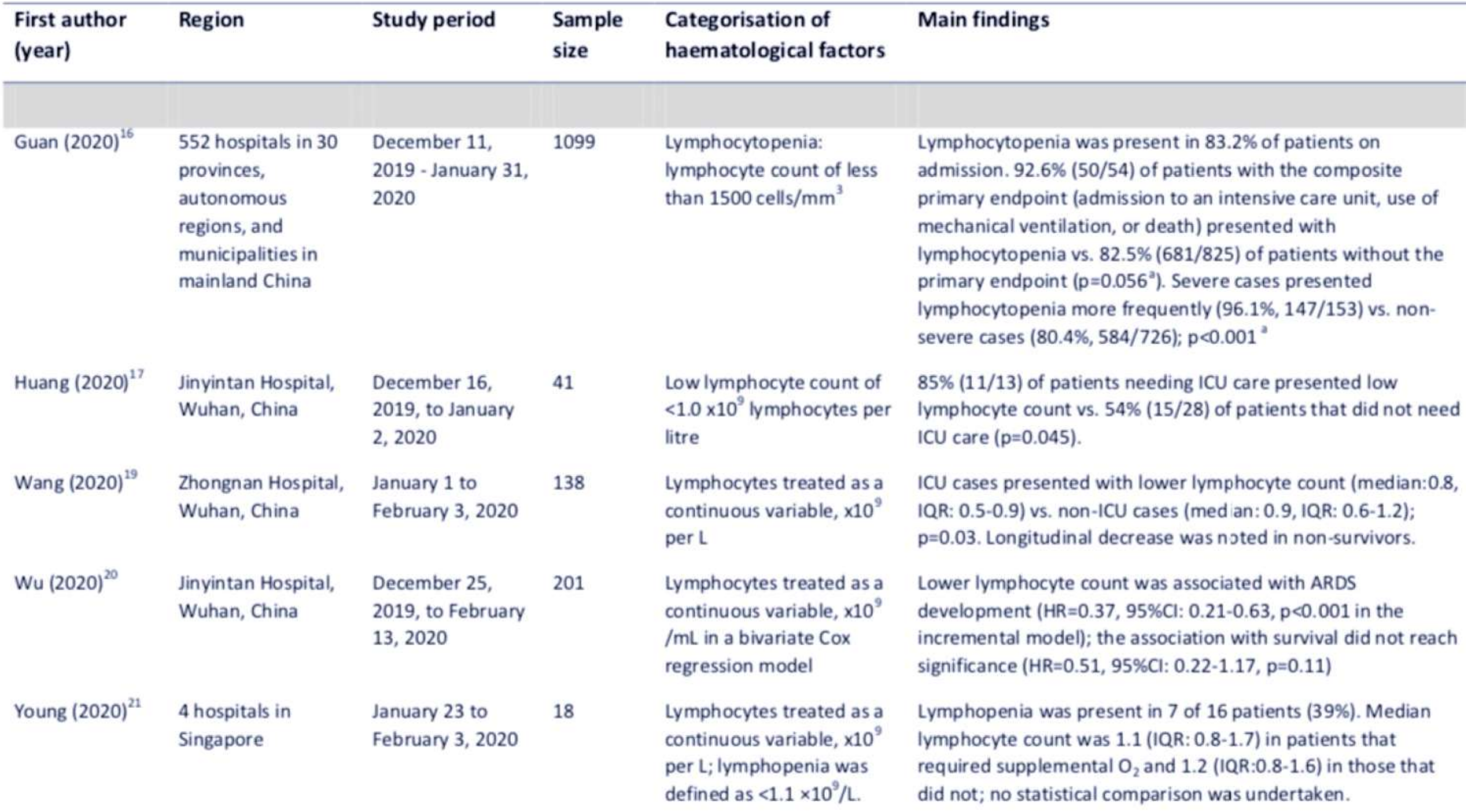

First author (year)	Region	Study period	Sample size	Categorisation of haematological factors	Main findings
Guan (2020)[16]	552 hospitals in 30 provinces, autonomous regions, and municipalities in mainland China	December 11, 2019 - January 31, 2020	1099	Lymphocytopenia: lymphocyte count of less than 1500 cells/mm^3	Lymphocytopenia was present in 83.2% of patients on admission. 92.6% (50/54) of patients with the composite primary endpoint (admission to an intensive care unit, use of mechanical ventilation, or death) presented with lymphocytopenia vs. 82.5% (681/825) of patients without the primary endpoint (p=0.056[a]). Severe cases presented lymphocytopenia more frequently (96.1%, 147/153) vs. non-severe cases (80.4%, 584/726); $p<0.001$ [a]
Huang (2020)[17]	Jinyintan Hospital, Wuhan, China	December 16, 2019, to January 2, 2020	41	Low lymphocyte count of $<1.0 \times 10^9$ lymphocytes per litre	85% (11/13) of patients needing ICU care presented low lymphocyte count vs. 54% (15/28) of patients that did not need ICU care (p=0.045).
Wang (2020)[19]	Zhongnan Hospital, Wuhan, China	January 1 to February 3, 2020	138	Lymphocytes treated as a continuous variable, $\times 10^9$ per L	ICU cases presented with lower lymphocyte count (median:0.8, IQR: 0.5-0.9) vs. non-ICU cases (median: 0.9, IQR: 0.6-1.2); p=0.03. Longitudinal decrease was noted in non-survivors.
Wu (2020)[20]	Jinyintan Hospital, Wuhan, China	December 25, 2019, to February 13, 2020	201	Lymphocytes treated as a continuous variable, $\times 10^9$ /mL in a bivariate Cox regression model	Lower lymphocyte count was associated with ARDS development (HR=0.37, 95%CI: 0.21-0.63, $p<0.001$ in the incremental model); the association with survival did not reach significance (HR=0.51, 95%CI: 0.22-1.17, p=0.11)
Young (2020)[21]	4 hospitals in Singapore	January 23 to February 3, 2020	18	Lymphocytes treated as a continuous variable, $\times 10^9$ per L; lymphopenia was defined as $<1.1 \times 10^9$/L.	Lymphopenia was present in 7 of 16 patients (39%). Median lymphocyte count was 1.1 (IQR: 0.8-1.7) in patients that required supplemental O_2 and 1.2 (IQR:0.8-1.6) in those that did not; no statistical comparison was undertaken.

Blood routine parameters of patients with COVID-19 on admission.

	Median (IQR)		
	All patients (n = 116)	Controls (n = 100)	*P* value
Age, Median(IQR),Range, years	50.0 (41.0–57.0), 20–93	48.5(37.3–59.8), 21–90	0.397
Sex			0.739
Male(%)	60 (51.7%)	53 (53.0%)	
Female(%)	56 (48.3%)	47 (47.0%)	
Blood routine			
Leucocytes($\times 10^9$ per L)	4.60 (3.76–6.40)	5.95 (5.13–6.88)	< 0.001
Neutrophils($\times 10^9$ per L)	3.10 (2.33–4.30)	3.20 (2.70–3.88)	0.456
Lymphocytes($\times 10^9$ per L)	1.00 (0.72–1.40)	2.10 (1.80–2.40)	< 0.001
Monocyte($\times 10^9$ per L)	0.39 (0.29–0.49)	0.40 (0.34–0.47)	0.372
Eosinophil($\times 10^9$ per L)	0.02 (0.01–0.05)	0.10 (0.06–0.16)	< 0.001
Hemoglobin(g/L)	132.5 (122.3–145.8)	146.5 (135.0–156.0)	< 0.001
Platelet($\times 10^9$ per L)	180.5 (145.5–229)	240.0 (202.8–274.8)	< 0.001
MLR	0.37 (0.27–0.56)	0.19 (0.17–0.23)	< 0.001
NLR	2.91 (1.87–4.83)	1.58 (1.34–1.98)	< 0.001
PLR	169.0 (123.5–245.6)	113.0 (95.1–138.2)	< 0.001

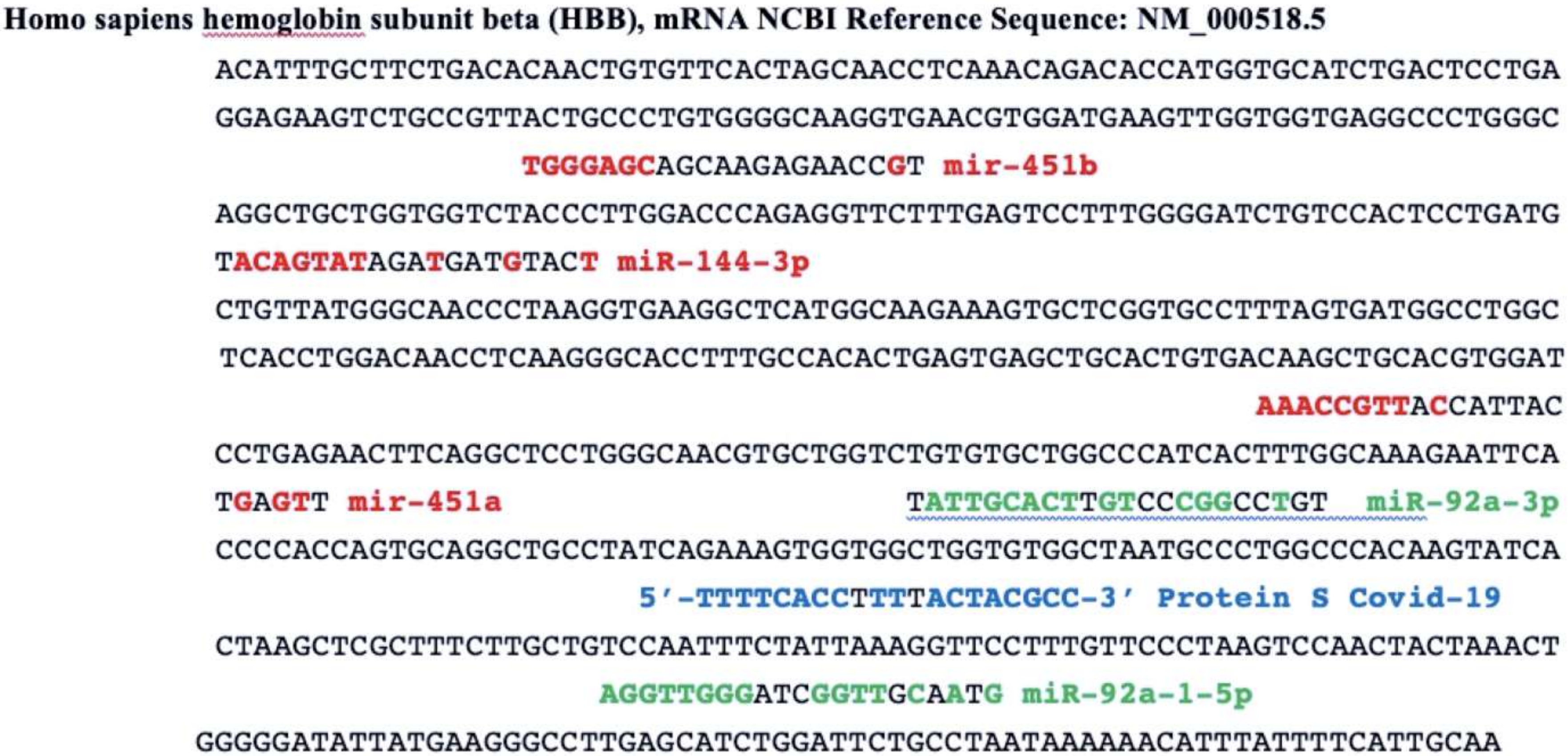

Homo sapiens hemoglobin subunit beta (HBB), mRNA NCBI Reference Sequence: NM_000518.5

```
ACATTTGCTTCTGACACAACTGTGTTCACTAGCAACCTCAAACAGACACCATGGTGCATCTGACTCCTGA
GGAGAAGTCTGCCGTTACTGCCCTGTGGGGCAAGGTGAACGTGGATGAAGTTGGTGGTGAGGCCCTGGGC
               TGGGAGCAGCAAGAGAACCGT mir-451b
AGGCTGCTGGTGGTCTACCCTTGGACCCAGAGGTTCTTTGAGTCCTTTGGGGATCTGTCCACTCCTGATG
TACAGTATAGATGATGTACT miR-144-3p
CTGTTATGGGCAACCCTAAGGTGAAGGCTCATGGCAAGAAAGTGCTCGGTGCCTTTAGTGATGGCCTGGC
TCACCTGGACAACCTCAAGGGCACCTTTGCCACACTGAGTGAGCTGCACTGTGACAAGCTGCACGTGGAT
                                                       AAACCGTTACCATTAC
CCTGAGAACTTCAGGCTCCTGGGCAACGTGCTGGTCTGTGTGCTGGCCCATCACTTTGGCAAAGAATTCA
TGAGTT mir-451a                       TATTGCACTTGTCCCGGCCTGT  miR-92a-3p
CCCCACCAGTGCAGGCTGCCTATCAGAAAGTGGTGGCTGGTGTGGCTAATGCCCTGGCCCACAAGTATCA
                     5'-TTTTCACCTTTTACTACGCC-3' Protein S Covid-19
CTAAGCTCGCTTTCTTGCTGTCCAATTTCTATTAAAGGTTCCTTTGTTCCCTAAGTCCAACTACTAAACT
                    AGGTTGGGATCGGTTGCAATG miR-92a-1-5p
GGGGGATATTATGAAGGGCCTTGAGCATCTGGATTCTGCCTAATAAAAAACATTTATTTTCATTGCAA
```

Figure 2. Human beta-globin gene [24] potentially targeted by a subsequence from Covid-19 protein S [23] (in blue), by microRNA miR-93a known for inhibiting its translation [25] (in green) and by microRNAs involved in erythrocyte maturation [26-31] (in red).

Genetic origin of Covid-19

The coronavirus isolated in pangolin is capable of entering human cells, while that isolated in the bat R. affinis is not. Furthermore, this suggests that the SARS-Cov-2 virus is the result of a recombination between two different viruses, one close to RaTG13 and the other closer to that of pangolin. In other words, it is a chimera between two preexisting viruses.

This recombination mechanism had already been described in coronaviruses, in particular to explain the origin of SARS-Cov. It is important to know that recombination results in a new virus potentially capable of infecting a new host species. For recombination to occur, the two divergent viruses must have infected the same organism concomitantly.

Two questions remain unanswered: in which organism did this recombination take place? (a bat, a pangolin or another species?) And above all, under what conditions did this recombination take place?

https://www.santemagazine.fr/actualites/actualites-sante/covid-19-lanalyse-des-genomes-revelerait-une-origine-double-du-virus-432862

Dependence on age-structure of the susceptible population

Covid-19 dynamics depends on age

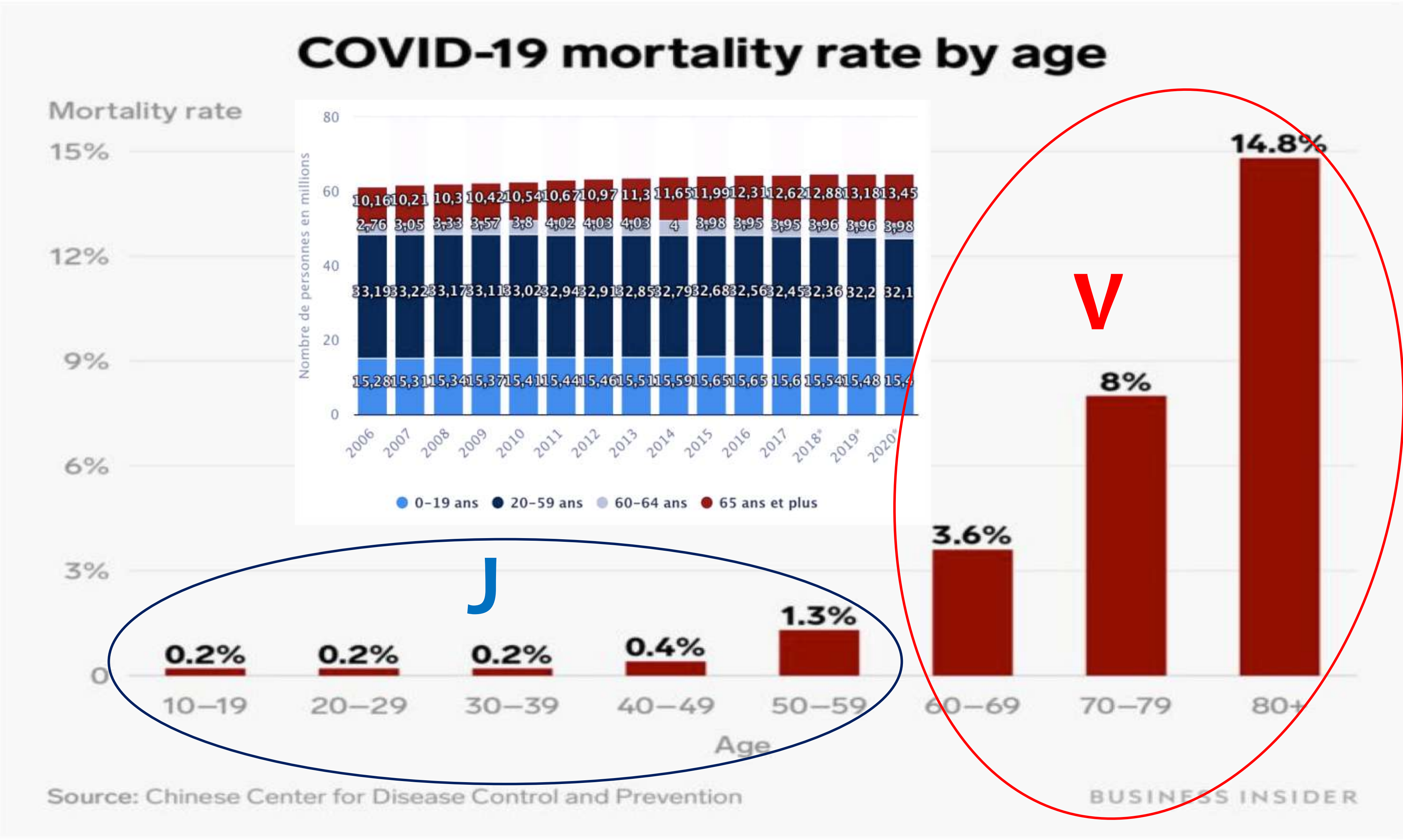

COVID-19 mortality rate by age

Source: Chinese Center for Disease Control and Prevention

Shayanne Gal/Business Insider

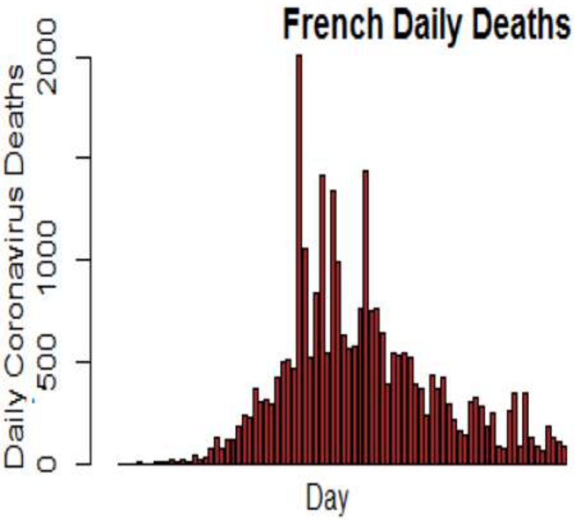

French Daily Deaths

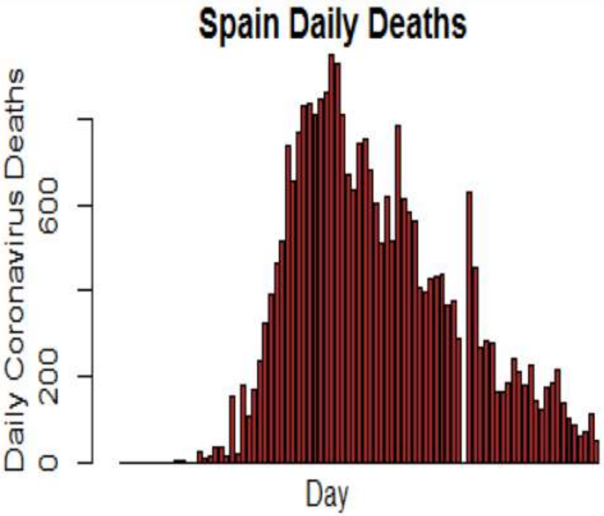

Spain Daily Deaths

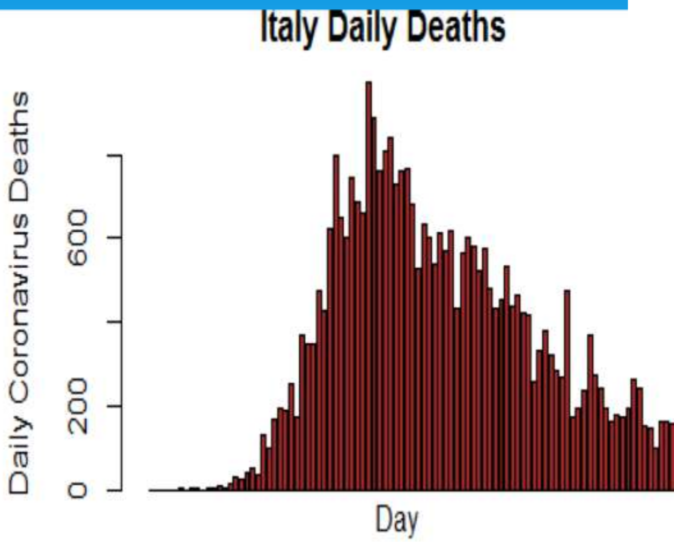

Italy Daily Deaths

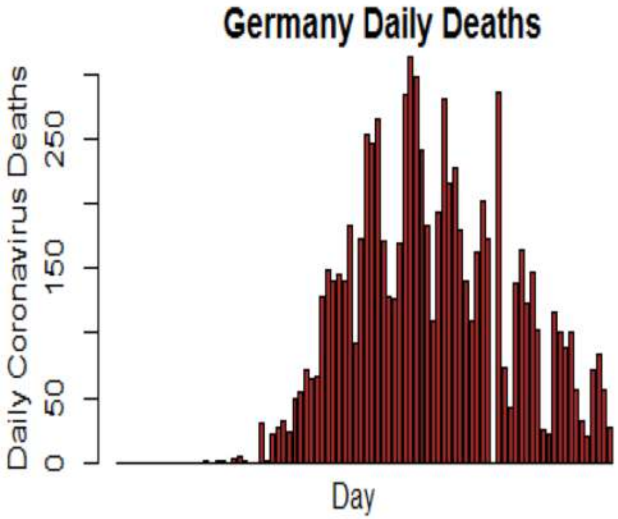

Germany Daily Deaths

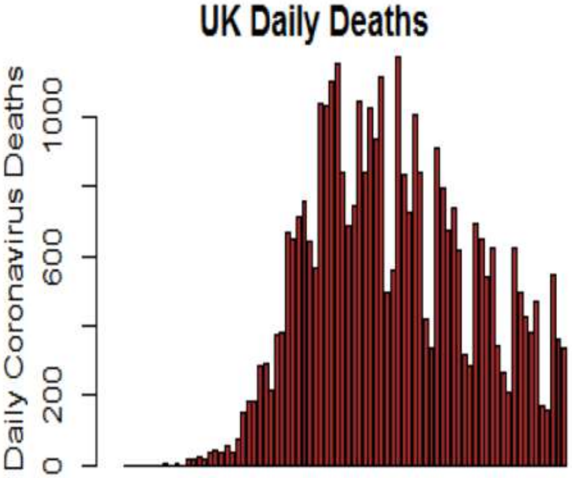

UK Daily Deaths

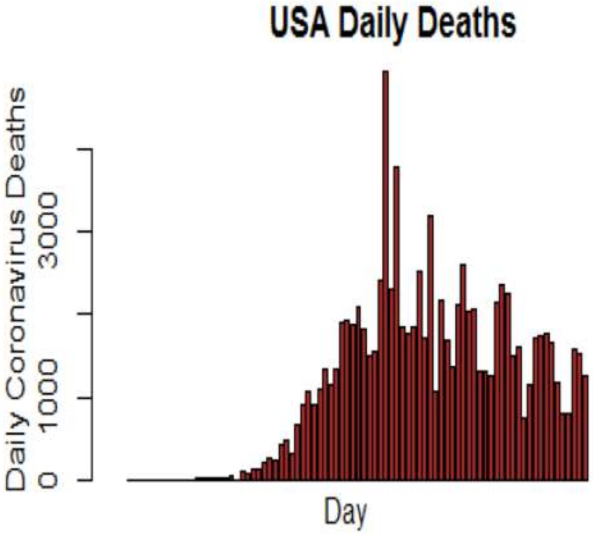

USA Daily Deaths

$$dS_1/dt = -ß_1*S_1*I_1 -ß_2*S_1*I_2 + k_1*R_1$$

$$dI_1/dt = ß_1*S_1*I_1 + ß_2*S_1*I_2 -(1-\mu_1)*I -\mu_1*I_1$$

$$dR_1/dt = (1-\mu_1)*I_1 -k_1*R_1$$

$$dS_2/dt = -ß_1*S_2*I_1 -ß_2*S_2*I_2 + k_2*R_2$$

$$dI_2/dt = ß_1*S_2*I_1 + ß_2*S_2*I_2 -(1-\mu_2)*I_2 -\mu_2*I_2$$

$$dR /dt = (1-\mu)*I -k *R$$

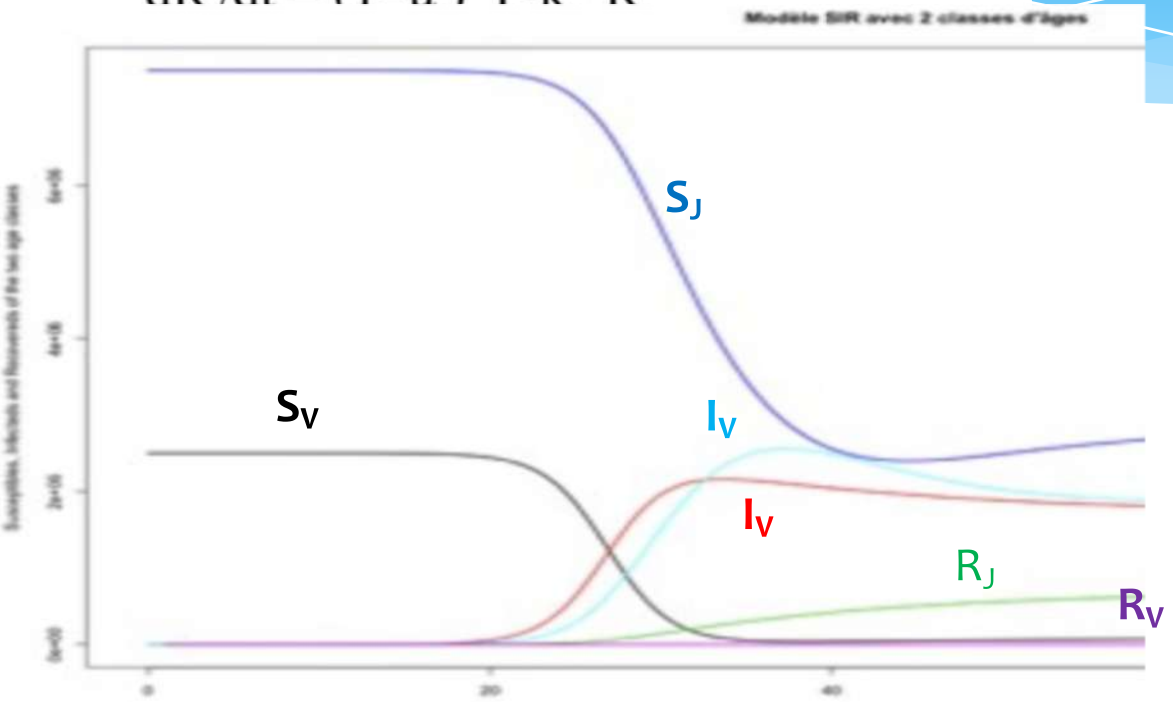

J. Demongeot, O. Hansen, H. Hessami, A.S. Jannot, J. Mintsa, M. Rachdi & C. Taramasco Random modelling of contagious diseases. *Acta Biotheoretica*, **61**, 141-172 (2013).

I. Ouassou, M. Rachdi, J. Demongeot. Covid-19 age-dependent dynamics. *Biology* (submitted).

Cross dependencies

Cheikh Faye[1], Cheikh Tidiane Wade[2], Ibrahima Demba Dione
A DISSYMMETRY IN THE FIGURES RELATED TO THE COVID-19 PANDEMIC IN THE WORLD: WHAT FACTORS EXPLAIN THE DIFFERENCE BETWEEN AFRICA AND THE REST OF THE WORLD?
medRxiv preprint doi: https://doi.org/10.1101/2020.05.17.20104687.May 22, 2020.

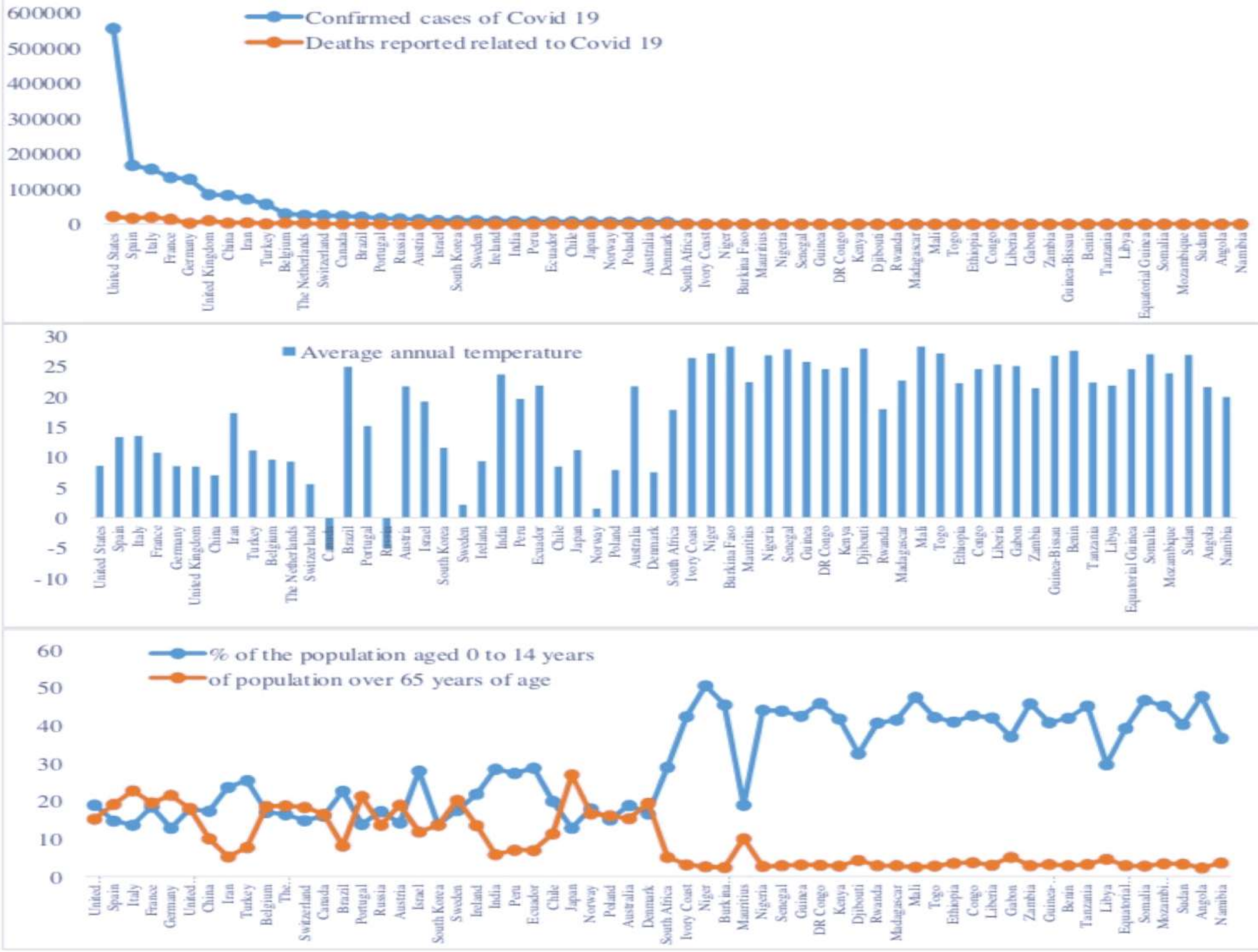
600000
500000
400000
300000
200000
100000
0
Confirmed cases of Covid 19
Deaths reported related to Covid 19
United States
Spain
Italy
France
Germany
United Kingdom
China
Iran
Turkey
Belgium
The Netherlands
Switzerland
Canada
Brazil
Portugal
Russia
Austria
Israel
South Korea
Sweden
Ireland
India
Peru
Ecuador
Chile
Japan
Norway
Poland
Australia
Denmark
South Africa
Ivory Coast
Niger
Burkina Faso
Mauritius
Nigeria
Senegal
Guinea
DR Congo
Kenya
Djibouti
Rwanda
Madagascar
Mali
Togo
Ethiopia
Congo
Liberia
Gabon
Zambia
Guinea-Bissau
Benin
Tanzania
Libya
Equatorial Guinea
Somalia
Mozambique
Sudan
Angola
Namibia
30
25
20
15
10
5
0
-5
-10
Average annual temperature
United States
Spain
Italy
France
Germany
United Kingdom
China
Iran
Turkey
Belgium
The Netherlands
Switzerland
Brazil
Portugal
Austria
Israel
South Korea
Sweden
Ireland
India
Peru
Ecuador
Chile
Japan
Norway
Poland
Australia
Denmark
South Africa
Ivory Coast
Niger
Burkina Faso
Mauritius
Nigeria
Senegal
Guinea
DR Congo
Kenya
Djibouti
Rwanda
Madagascar
Mali
Togo
Ethiopia
Congo
Liberia
Gabon
Zambia
Guinea-Bissau
Benin
Tanzania
Libya
Equatorial Guinea
Somalia
Mozambique
Sudan
Angola
Namibia
60
50
40
30
20
10
0
% of the population aged 0 to 14 years
of population over 65 years of age
United...
Spain
Italy
France
Germany
United...
China
Iran
Turkey
Belgium
The...
Switzerland
Canada
Brazil
Portugal
Russia
Austria
Israel
South Korea
Sweden
Ireland
India
Peru
Ecuador
Chile
Japan
Norway
Poland
Australia
Denmark
South Africa
Ivory Coast
Niger
Burkina...
Mauritius
Nigeria
Senegal
Guinea
DR Congo
Kenya
Djibouti
Rwanda
Madagascar
Mali
Togo
Ethiopia
Congo
Liberia
Gabon
Zambia
Guinea-...
Benin
Tanzania
Libya
Equatorial...
Somalia
Mozambi...
Sudan
Angola
Namibia

Other dependencies

H. Seligmann, S. Iggui, M. Rachdi, N. Vuillerme & J. Demongeot
Inverted covariate effects for mutated 2nd vs 1st wave Covid-19: high temperature spread biased for young.
Biology (Basel) (submitted).

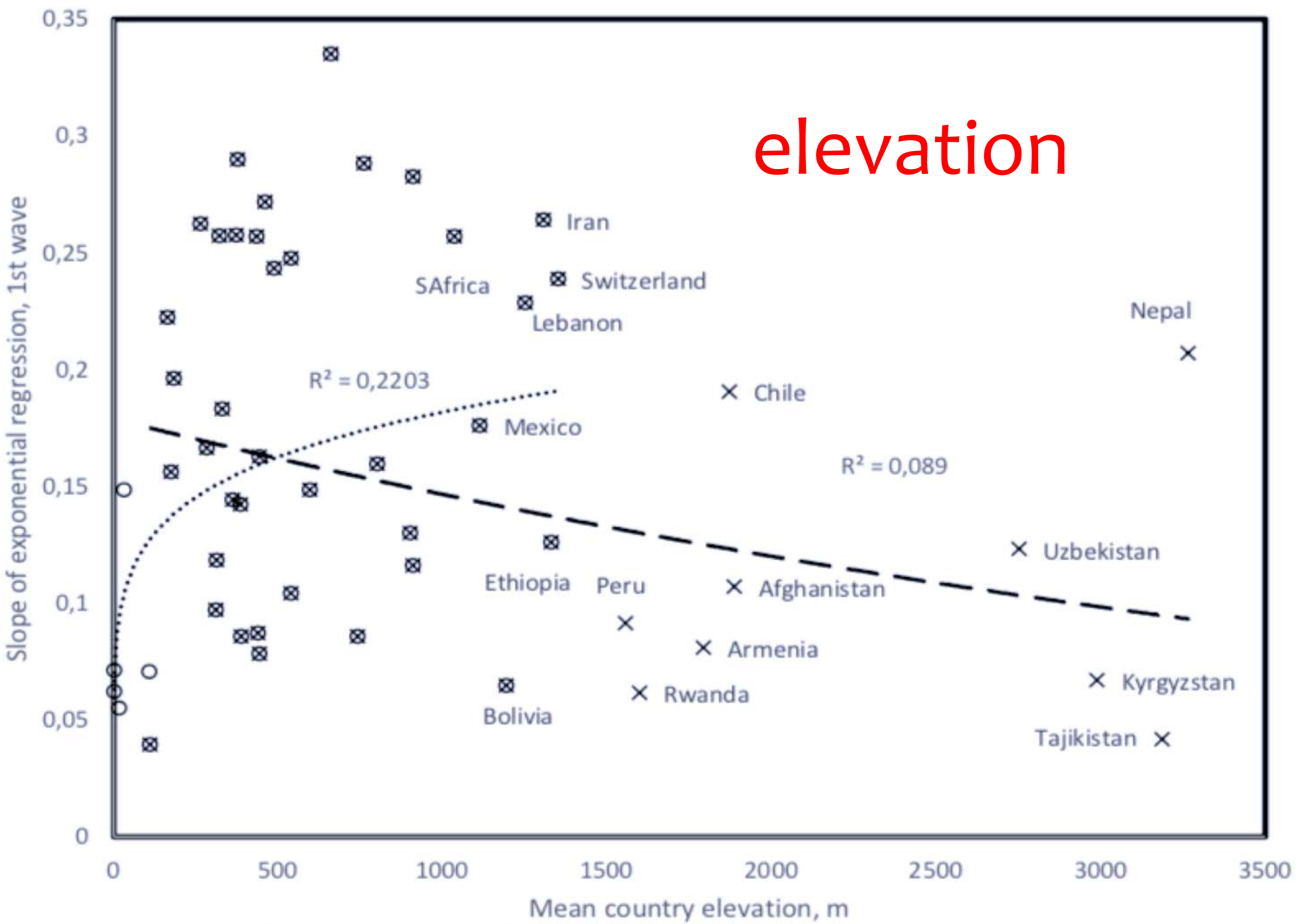

Figure 1. Slope of daily new confirmed Covid-19 cases as a function of mean country elevation. Circles: Countries contributing to the positive trend with elevation, up to 1400m, r = 0.469, two tailed P = 0.0015;

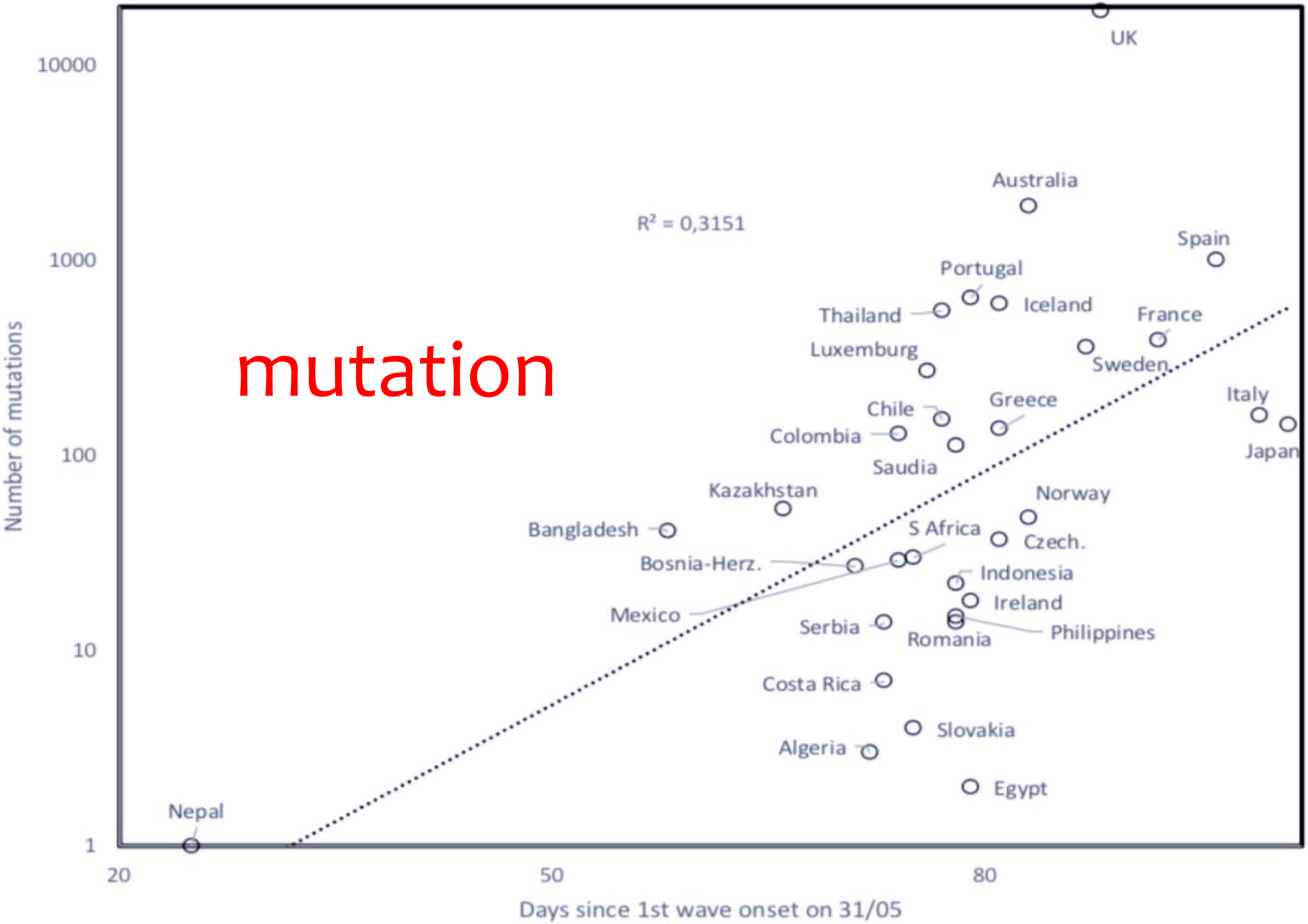

Figure 2. Mutation numbers as a function of days since onset of 1st wave (determined on 31/05).

2^{nd} wave

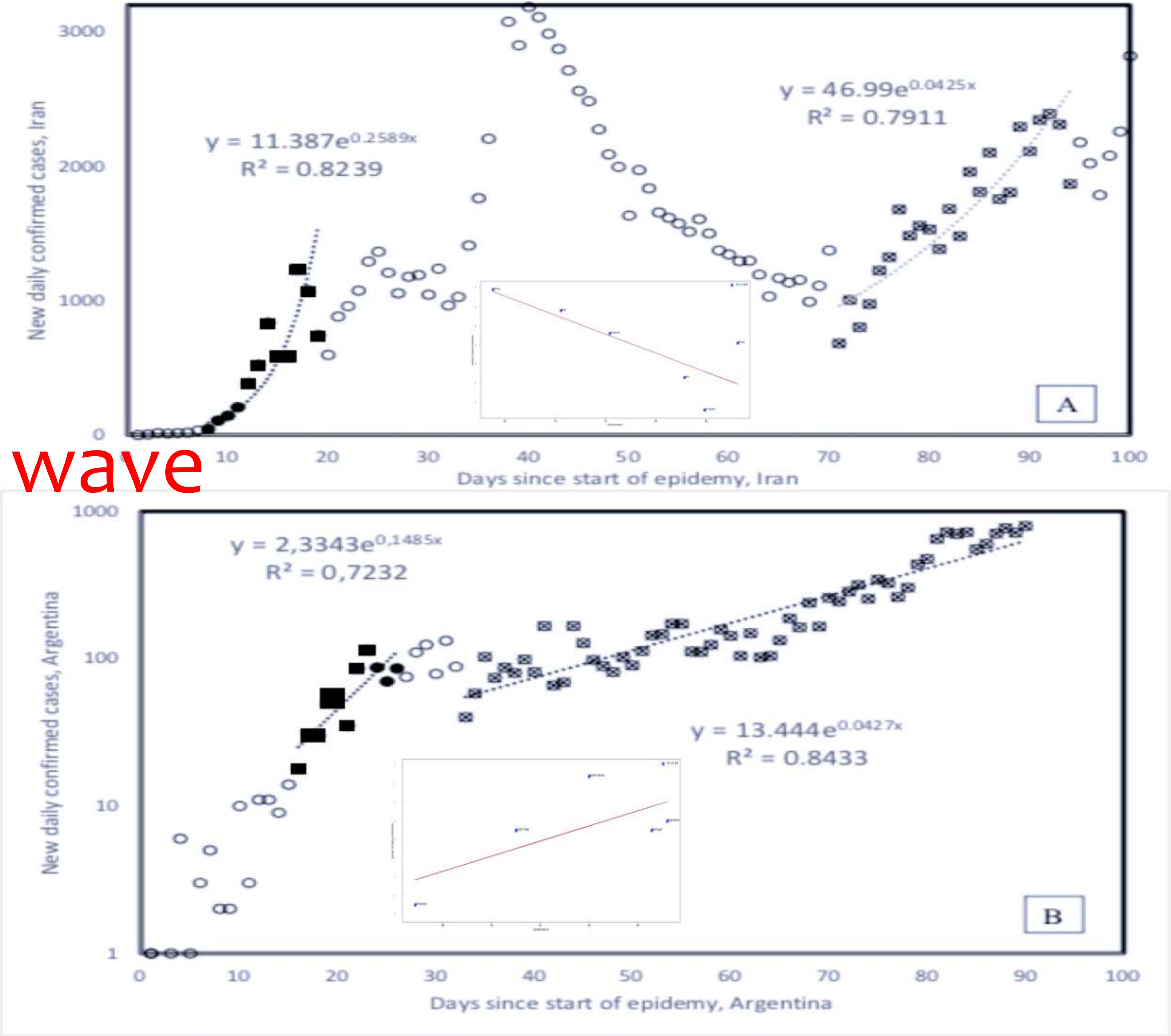

Figure 3. 1st and 2nd waves of Covid-19 epidemy in Iran (A) and Argentina (B). 1st wave onsets are

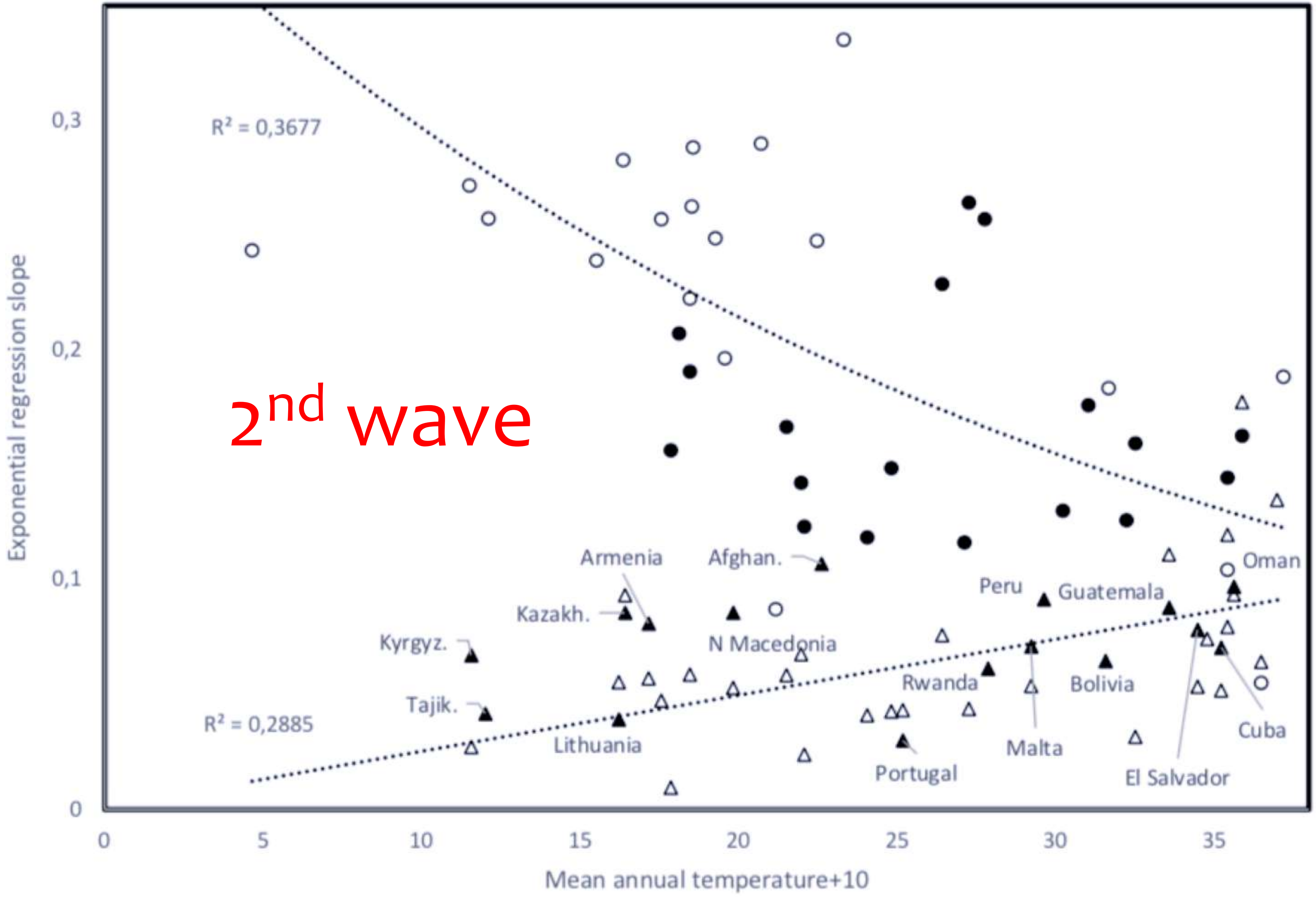

Figure 4. Slope of exponential regression of daily new cases vs time, as a function of mean annual temperature, comparing trends for 1st wave slopes (open circles from [1], filled circles and triangles are from this study), and 2nd wave slopes (open triangles).

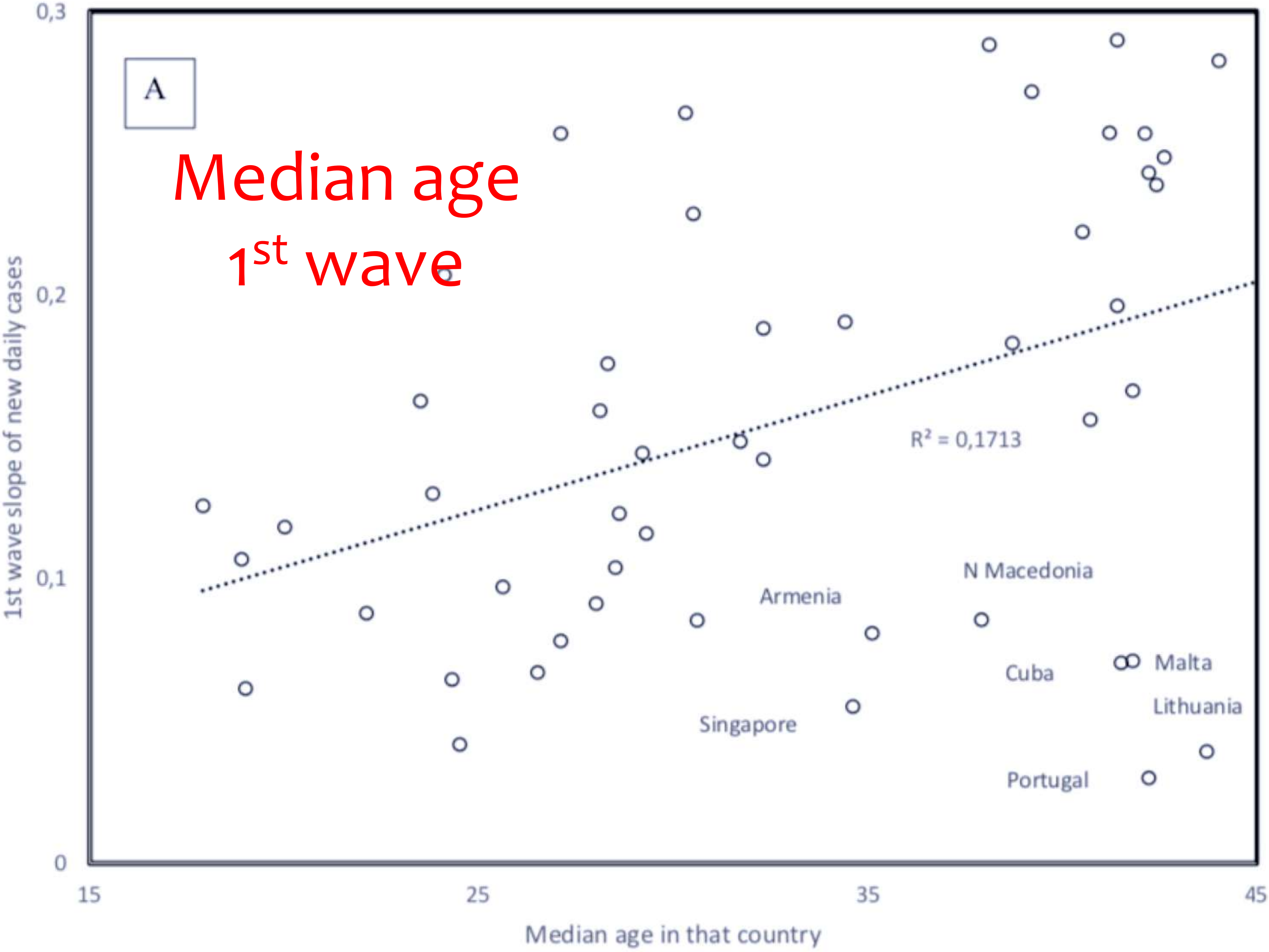

Median age
1st wave

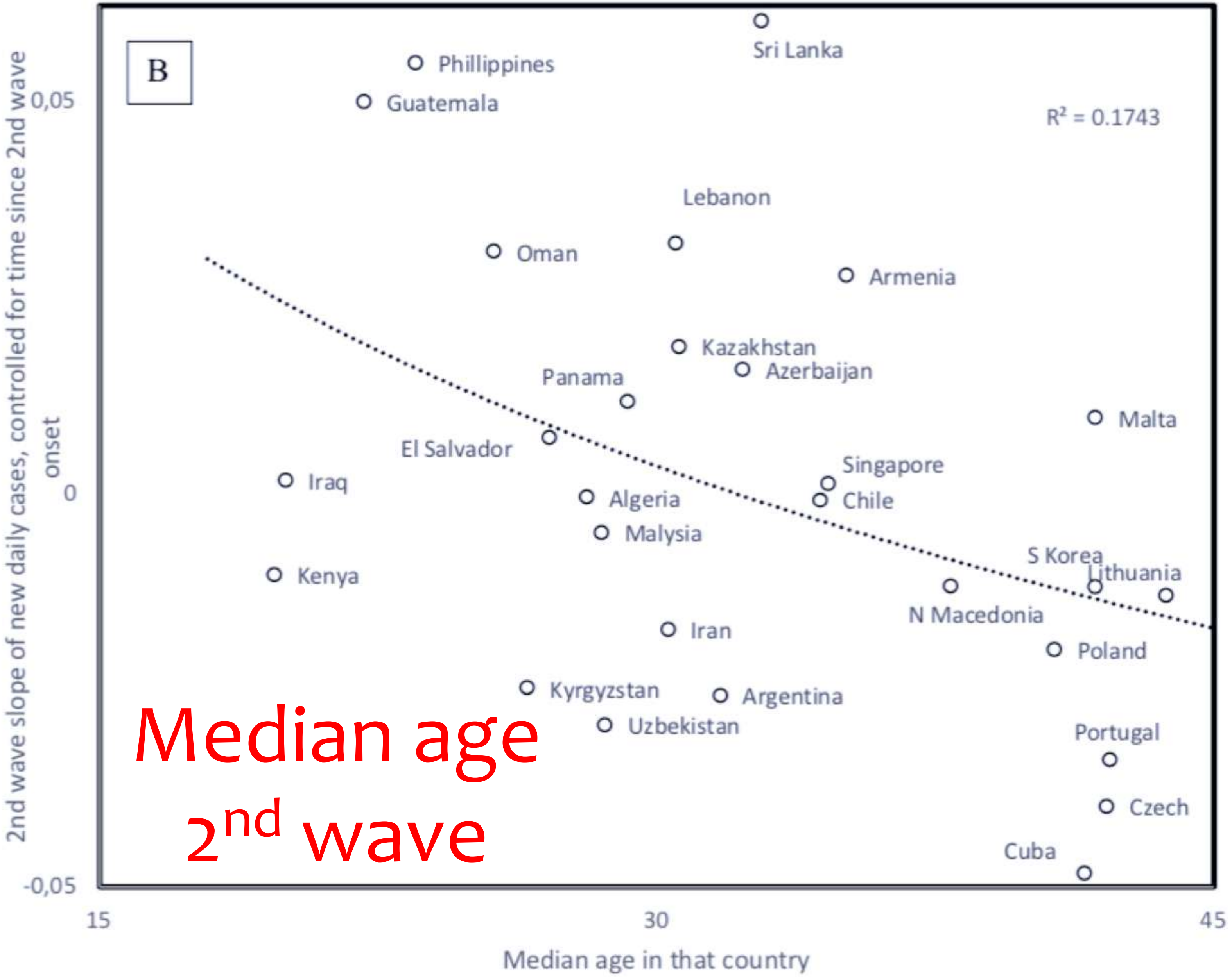

Median age
2nd wave

Figure 6. 1st (A) and 2nd (B) wave slopes as a function of country median age. For 2nd wave slopes, the figure plots the residual values after adjusting 2nd wave slopes for time since 2nd wave start (regression in Figure 4B), the main correlate of 2nd wave slopes.

Merci pour votre attention !

- NB Pierre Magal and myself are responsible of a peer-reviewed special issue on covid-19 modelling in *Biology*, Section Theoretical Biology in which you are invited to publish: www.mdpi.com/journal/biology/special_issues/COVID-19_Epidemic